Department of Justice, Office of Justice Programs

National Institute of Justice

Grant # 2018-DU-BX-0180

The Impact of Drugs on Human Decomposition and the Postmortem Interval: Insect, Scavenger and Microbial Evidence

Final Report

Project Period January 1, 2019 – July 31, 2021

$726,629

Submitted by:

Dawnie Wolfe Steadman, Ph.D., D-ABFA
Chancellor's Professor, Department of Anthropology
865-974-0909; osteo@utk.edu

Jennifer DeBruyn, Ph.D.
Associate Professor, Biosystems Engineering and Soil Science
(865) 974-7277; jdebruyn@utk.edu

Shawn Campagna, Ph.D.
Professor, Department of Chemistry
865-974-3141; campagna@utk.edu

Kristi Bugajski, Mary Davis, Thomas Delgado, Katharina Höland, Allison Mason, Amanda May, Hayden McKee, Charity Owings, Erin Patrick, Sarah Schwing

DUNS: [redacted]
EIN: [redacted]

The University of Tennessee
1 Circle Park Drive
Knoxville, TN 37996-0003

Table of Contents

List of Figures

List of Tables

Project Summary

The Forensic Anthropology Center at the University of Tennessee has been the leader in human decomposition research at the Anthropology Research Facility (ARF), or "Body Farm," for over forty years. The majority of decomposition research has focused on how environmental factors, such as temperature, insect activity, sunlight, clothing and wrappings, soil chemistry and microbes affect decomposition rates (e.g., Damann et al. 2015; Mann et al. 1990; Rodriguez and Bass, 1983; Rodriguez and Bass, 1985; Vass et al. 1992; Wilson-Taylor and Dautartas, 2017). Recently, however, researchers conducted a series of trials with multiple donors placed simultaneously in the same microenvironment at the ARF (3-5m apart) and observed differential decomposition. Specifically, some donors were heavily scavenged while others were completely ignored by scavengers, insect colonization times varied despite identical external environments, and even soil chemistry profiles differed between individuals (Dautartas et al. 2018; Steadman et al. 2018; DeBruyn et al. 2021). It seems, therefore, that characteristics of the deceased body itself may enhance or disrupt decomposition progression such that time since death estimates based on human morphology or entomological evidence could carry unquantified error. The purpose of this study is to systematically examine if and how the body exerts agency over its own decomposition process by studying the effects of drugs and end of life diseases on decomposition rates and patterns.

Use of prescription medications as well as drugs of abuse has risen 30% worldwide between 2009 and 2018, and the drug overdose rate in the United States increased nearly 10% in a single year (2016-2017) (U.N. World Drug Report, 2021). While illicit drug use also has increased, almost half of all opioid-related overdoses are attributed to prescription sources, a rate that has quadrupled since 1999 and increasingly affects the elderly (National Institute on Drug Abuse, 2020; CDC 2017:25). Beyond the opioid epidemic, however, pharmaceutical dependence tracks

U.S. morbidity and mortality trends, where seven of the top 10 causes of death in the U.S. in 2019 (prior to the emergence of SARS-CoV-2) were chronic diseases requiring pharmaceutical intervention, including heart disease, cancer, chronic lower respiratory diseases, stroke, Alzheimer's, diabetes, and other kidney diseases (Kochanek et al. 2020). Medication use is not restricted to older adults as children are also high consumers of antibiotics, asthma medication (steroids), and behavior/mood altering drugs (Chai et al. 2012; Hales et al. 2018; Visser et al. 2014). Estimates of "long-haul disease" in over one-third of Covid-19 patients will also necessitate long-term medications even for those who were once healthy (Huang et al. 2021). The permanence of drugs (hereafter to include both illicit drugs and prescribed or over-the-counter medications) in daily American life means that most death investigations will involve decedents who have drugs in their system. An important forensic question, then, is whether pathological conditions and/or the drugs used for treatment (or drugs of abuse) alter expected decomposition rates of the body and introduce unknown error to morphological and entomological estimates of the postmortem interval (PMI). Hayman and Oxenham (2016) evaluated two human subjects that differed in medical treatment (cancer and diabetes/heart attack) before death, and the results of this work suggested that perimortem medical treatments can have significant effects on decomposition rates and patterns. To address this issue, we study a larger number of donors and combine taphonomic observations with cutting edge -omics approaches to examine how drugs and diseases suffered by donors at the end of their life impact the primary decomposers – insects, scavengers, enteric bacteria and soil microbes.

Studies of pharmaceuticals and drugs of abuse in animal carcasses have clearly shown that drugs differentially affect the timing of insect life cycles (e.g., Goff et al 1989; Kintz 1990, Bourel et al. 2001). For instance, maggots reared on organs of rabbits injected with diazepam exhibited

increased growth rates and altered pupa morphology compared to controls (Carvalho et al. 2001). Pharmaceuticals can also significantly alter the composition and functioning of our gut microbiota (Fuyuan 2016, Banarjee 2016). Research on application of human or animal wastes (e.g. biosolids or reclaimed water) to land has demonstrated that the antibiotics and pharmaceuticals found in these wastes can significantly alter soil microbial communities (Qin et al. 2015, Caracciolo et al. 2015); thus, it is highly plausible that drugs or drug metabolites found in decomposing bodies would affect the environmental microbiota in this system. Since insects and both the internal and external microbiomes mediate decomposition, a change in these communities could ultimately influence the rate or trajectories of decomposition. Finally, no studies have explicitly correlated scavenger choice in consumption of human body tissues with individuals of documented diseases, treatments, and multiple drugs in their system.

This longitudinal study of human donors with known disease and drug histories examines whether drugs and their metabolic products impact the physiology, behavior, and/or community composition on the three primary groups of decomposers (insects, scavengers, and microbes) and correlate these with observed decomposition rates (Figure 1). We applied multi-omics approaches to determine whether drugs lead to a detectable shift in the metabolome and microbiome of human donors that will then impact the behavior and/or physiology of organisms that use the human body as a food source. Our data will ultimately inform if and how postmortem interval (PMI) estimates should be modified when certain drugs are present and assess the need to perform toxicological testing of different matrices prior to PMI estimation.

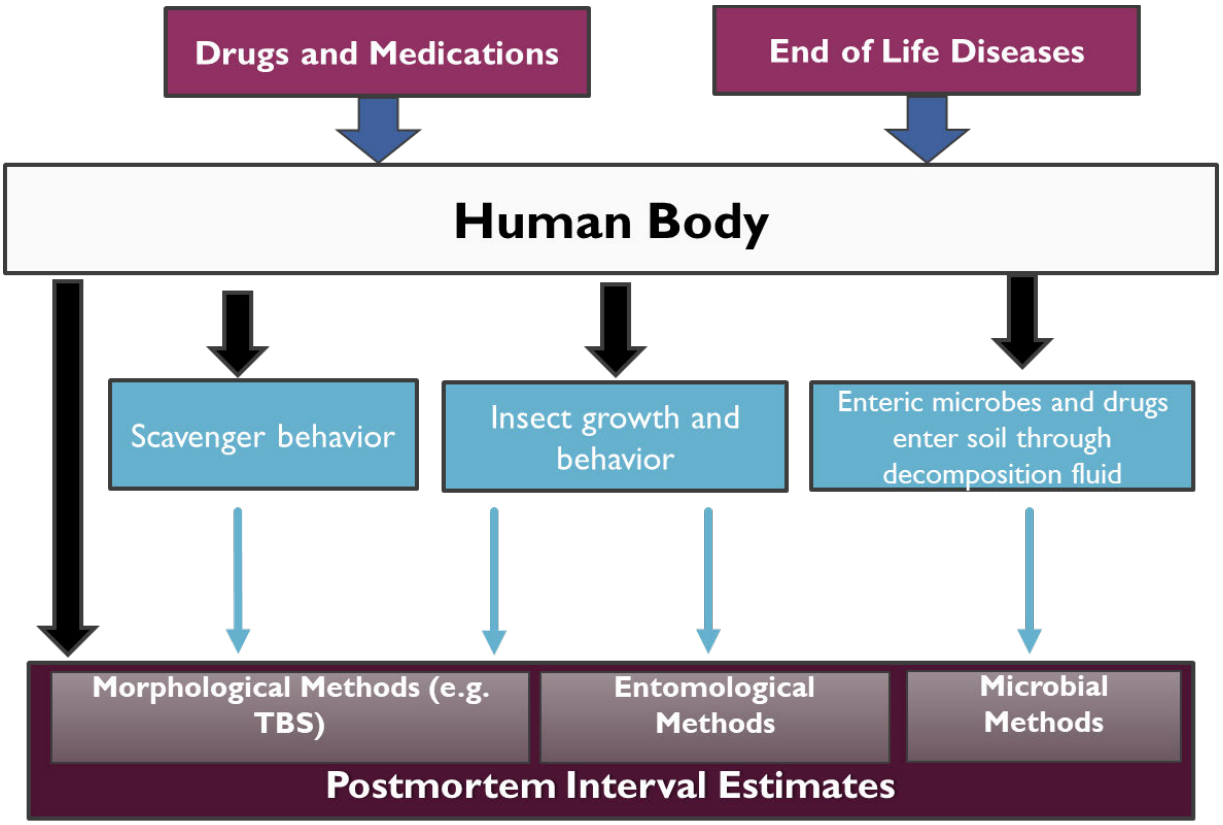

Figure 1. Relationship between drugs and end of life diseases and decomposers that may affect the postmortem interval estimate.

Goals and Objectives

The overall goal of this research project was to establish the relationship between human toxicological loading and decomposition dynamics. Our hypothesis was that multiple drug metabolites can influence the behaviors of these decomposers by changing the metabolite profile (the total metabolite content in the system) of the decomposing body and, thus, result in differential rates of decomposition. To test this hypothesis, we conducted metabolomic profiling, microbial DNA sequencing, and entomological identifications to carry out the following objectives:

1. Determine if the metabolites present in blood serum can be tracked across decomposer matrices.

This resource was prepared by the author(s) using Federal funds provided by the U.S. Department of Justice. Opinions or points of view expressed are those of the author(s) and do not necessarily reflect the official position or policies of the U.S. Department of Justice.

2. Determine the relationship between the drug metabolite profile of donated human subjects and the community structure and/or physiology of insects and microbes.

3. Determine the relationship between the metabolite profile of donated human subjects and the behavior of scavengers.

Research Design

Data Collection

Human subjects involved in this project were obtained through the Body Donation Program of the Forensic Anthropology Center (FAC). The FAC requested a list of medications and treatments given during the last two weeks of life as well as a description of the diseases and conditions at end of life. Donors without open wounds, and for whom femoral and aortic blood serum samples could be obtained, were enrolled and placed at the ARF for this longitudinal study. Baseline soil samples were taken at the placement site and at a control site approximately one meter away from the donor. A data logger was placed close to the donor to provide a localized hourly recording of temperature and relative humidity. These local temperatures were used to calculate the accumulated degree hours (ADH)[1] that served as a metric to determine sampling points for soil and decomposition fluid. Infrared motion sensing digital game cameras were set by each donor to collect images of any scavenger presence and activity on the bodies.

[1] Accumulated degree hours (ADH) and accumulated degree days (ADD) measure the thermal energy available to organisms over time. ADH for this study is calculated as the sum of hourly temperatures (minus 10°C) until unenrollment. ADD is calculated as the daily mean temperature above the threshold of 0°C until unenrollment.

Donor decomposition and insect and scavenger activity were documented twice daily with photographs and data collection forms. Table 1 provides the sampling strategy (by ADH) for all field data. Data collection techniques included:

- Decomposition fluid was collected when it was released from the donor and had sufficiently pooled on the ground surface within the cadaver decomposition island (CDI). The tip of a sterile 30-ml syringe was carefully inserted into the surface of the pooling fluid and slowly drawn up. This process was repeated until ten milliliters were collected. The syringe was inverted to mix and 1.75 ml dispensed into four 2-ml cryovials.
- Between five and eight soil cores were obtained at a depth of 5 cm using a sterile 10-ml syringe with the tip cut off. Soil cores were taken from adjacent to the donor and at a control point at least 1 m away from the donor. Soils were homogenized and debris larger than 2 mm (i.e. rocks, roots, insects, etc.) was removed.
- Larvae of all immature development stages (1st through post-feeding 3rd instars) were collected. Larvae collected for the purposes of morphological identification were immediately par-boiled and placed in 70% ethanol on-site. Flying adult insects were collected with an aerial sweep net, whereas non-flying adults were collected by hand when possible. All adult insects were killed and stored in 70% ethanol.
- Subsamples of larvae, soil and fluids were immediately flash frozen with liquid nitrogen in the field, stored in liquid nitrogen at the FAC and then regularly transported to the UTK Biological and Small Molecule Mass Spectrometry Core (BSMMSC) for targeted and untargeted analysis for metabolomic profiling as well as the Department of Biosystems Engineering & Soil Science for DNA profiling and sequencing.

Sampling was terminated when the trunk of the body no longer actively produced visible fluids rather than at a particular ADH marker. For instance, a donor assigned as Tox 007 stopped producing fluids and was removed from the study at 6000 ADH (Figure 1C), which occurred 19 days after placement, while Tox 001 continued in a state of active decay until 16,225 ADH, 93 days following placement.

Table 1. Description of project target samples and collection sites

Subject	Donors for whom serum and blood samples are available
Blood Samples	Central and peripheral serum and blood at intake
Photos, Scavenging and Insect Data	Twice daily. Scavenger data also collected via game cameras
Maggot Collection	Two vials collected from three separate body locations at four distinct ADH (24 vials/donor)
Soil and Decomposition Fluid	100, 250, 500, 750, 1000ADH then every 500 ADH until trunk ceases to release fluid; soil samples sequenced at ~1500, 3000 and 4500 ADH
TBS*	Scored from randomized weekly photos

* TBS is Total Body Score, a method to document morphological evidence of documentation throughout body regions and calculate an estimate of ADH, accumulated degree hours since placement

Figure 2: Donor Tox 007 at (A) 100 ADH a day after placement, (B) 2000 ADH seven days after placement, and (C) 6000 ADH, eighteen days after placement. It can be seen that at 2000 ADH (B) the body is still bloated and secreting visible fluid. The dry leather appearance of the trunk in (C) indicates that fluid is no longer being secreted under the skin and active decay has ceased. In contrast, Donor Tox 001 at 16,225 ADH (D) had only recently ceased producing fluid, shown here at 93 days after placement.

Laboratory Analysis

Postmortem toxicological analysis was performed on central and peripheral serum collected at intake using ultra-high-performance liquid chromatography–high-resolution mass spectrometry (UHPLC-HRMS). Stock solutions of commercial drug standards (Restek, Bellefonte, PA) containing 15 drugs from major pharmaceutical classes were used for validation of compound identity as well as quantitative analyses. Metabolites were extracted and targeted tandem mass spectrometric analyses were performed using an UPLC-Quadrupole/Orbitrap Q Exactive MS while untargeted, global metabolite analyses used an UPLC- Orbitrap Exactive MS. The untargeted metabolomics methods were able to simultaneously quantitate both the known metabolites and the molecules of undetermined structures ("unknowns"). All spectral profiles were filtered to remove peaks below an abundance threshold to lower the chances of including peaks that arose from random noise. Metabolite identification and annotation was performed using retention time and exact mass, as well as fragmentation data of lipids and larger metabolites.

Microbial DNA was extracted from all soil and decomposition fluid samples using the DNeasy Powerlyzer PowerSoil kit (QIAGEN Inc.). Soil was also analyzed using an Orion Star™ A329 multiparameter meter (Thermo Scientific) to measure pH and electrical conductivity (EC). Soil respiration was assessed as CO_2 evolved in a closed headspace after 24 hours at 20°C, measured using an Infrared Gas Analyzer (IRGA).

Dichotomous keys were used to determine the taxonomic classification of all 3rd instar larvae (Liu and Greenberg 1989, Szpila 2009) (larvae younger than 3rd instar cannot be reliably identified to genus or species) and all adults. Additionally, all sampled larvae were measured to the nearest 0.1 millimeter. In order to determine if there were any significant differences between the length of larvae present on each donor, 3rd instar larvae of the blow fly *Phormia regina* were used for

analysis as they were present on all but three donors. Intrinsic factors (including disease status and presence of pharmaceuticals) and environmental factors (e.g., temperature), were analyzed to determine their impact on the pre-colonization interval (pre-CI), or time interval between donor placement and initial blow fly colonization.

The time between placement and scavenging (if it occurred at all), frequency of scavenging events and extent of scavenging were evaluated from the morning and afternoon field notes and photographs. Evidence of scavenging modification on the donors included superficial scratching, penetration of the skin, tissue disruption, and consumption. Scavenger species were identified from the game camera images. The minimum number of scavenging sites (MNSS) represents the frequency of any scavenger alteration of the remains and is a measure of the extent of scavenging on each donor (Steadman et al. 2018).

Morphological changes during decomposition were documented from daily photos using Total Body Score (TBS) (Megyesi et al. 2005). The scoring method involves assigning incremental scores of decomposition, from fresh to skeletonized, for three regions of the body – head and neck, torso, and limbs – and then summed. The estimated ADD is then compared to the known ADD as determined from the time of placement to unenrollment.

Results

The analysis of multifactorial data (e.g., metabolomics, genomics, insect behavior, microbial community structures, soil chemistry, scavenging frequency) is complex and our work to assess statistical relationships is ongoing. While there are a number of important findings, we focus here on three key trends that will be analyzed further in upcoming publications. First, we document that drug metabolites detected from donor blood serum can be traced to insects and microbes. Second,

we found changes in community structure or physiological responses of insects and microbes that can be correlated with end of life diseases and/or their attendant drugs. Finally, we begin to explore the effects of drugs and diseases on decomposition rates and insect behavior that will ultimately affect PMI estimations. To demonstrate these findings, we first document the health and toxicological loads of the donors studied.

Donor Disease Loads and Toxicological Screening

Longitudinal data were collected for 22 donors. Appendix 1 provides the demographic and medical conditions for each donor as well as the medications reported to be taken within two weeks of death. Figure 3 demonstrates the drug classes represented as well as reported disease categories. All 22 donors had documented co-morbidities or risk factors (e.g., tobacco use), with cancer and respiratory diseases representing the most common disease conditions reported (Figure 4). All of the 17 donors for whom medication lists are available reported use of multiple drugs (between 3 and 24 drugs per donor), with a mean of 11 drugs per donor.

Figure 5 compares the drugs detected in the toxicological screenings to the drugs reportedly taken by each donor (n = 17). Approximately 54% of drugs on the provided medication lists were detected by the toxicological screenings. Moreover, the toxicological screenings detected approximately 35% more drugs than were listed on the medication lists. Of these, six drugs were detected but not reported by any donor – codeine, dihydrocodeine, meperidine, oxymorphone (all opioids), mirtazapine (anti-depressant), and promazine (anti-psychotic), while others were under-reported, such as acetaminophen (pain), morphine (opioid), citalopram (anti-depressant), and carbidopa-levodopa (Parkinsons). Duloxetine (an anti-depressant), was reported but not detected in in two cases, but this compound was detected in the sera of two other donors for whom it was not reported. Two donors (Tox 013 and Tox 022) died from acute trauma, rather than chronic end-

of-life diseases, yet multiple drugs were detected in their blood serum, demonstrating that even donors who did not have end-of-life diseases still had drugs in their systems at the time of death.

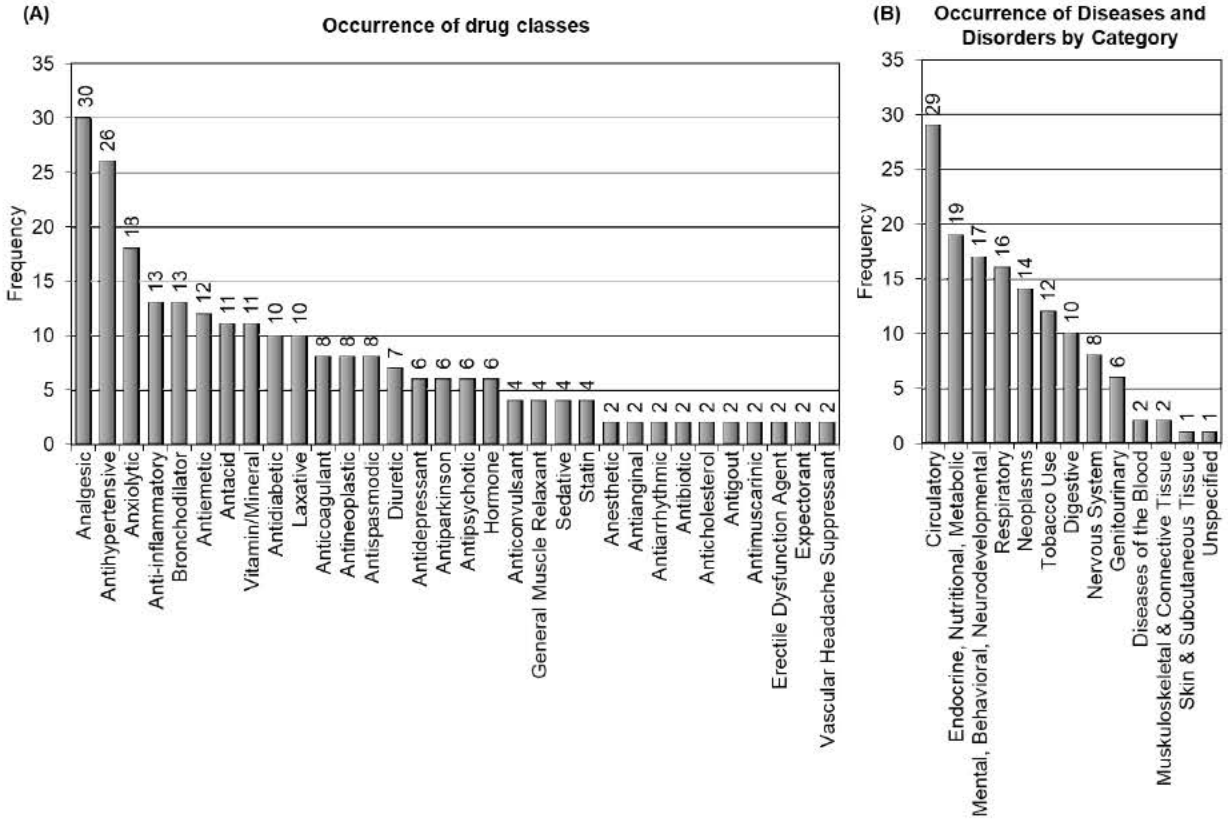

Figure 3. A) Frequency of reported drugs by category for 17 donors with medicine lists, and B) frequency of reported diseases and medical disorders by category for 22 donors. Note that donors have multiple diseases and drugs reported, each of which are compiled in these categories.

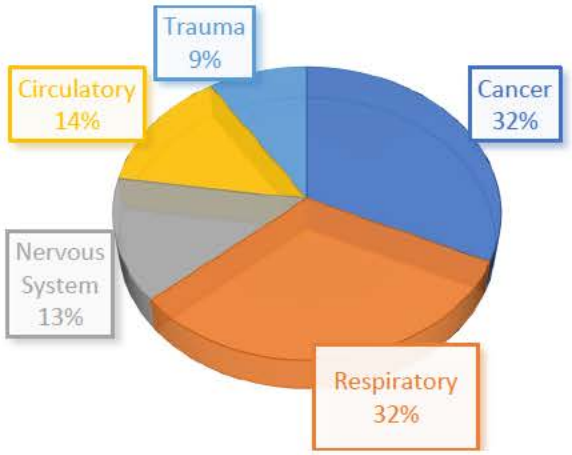

Figure 4. Frequency of cause of death categories for 22 donors.

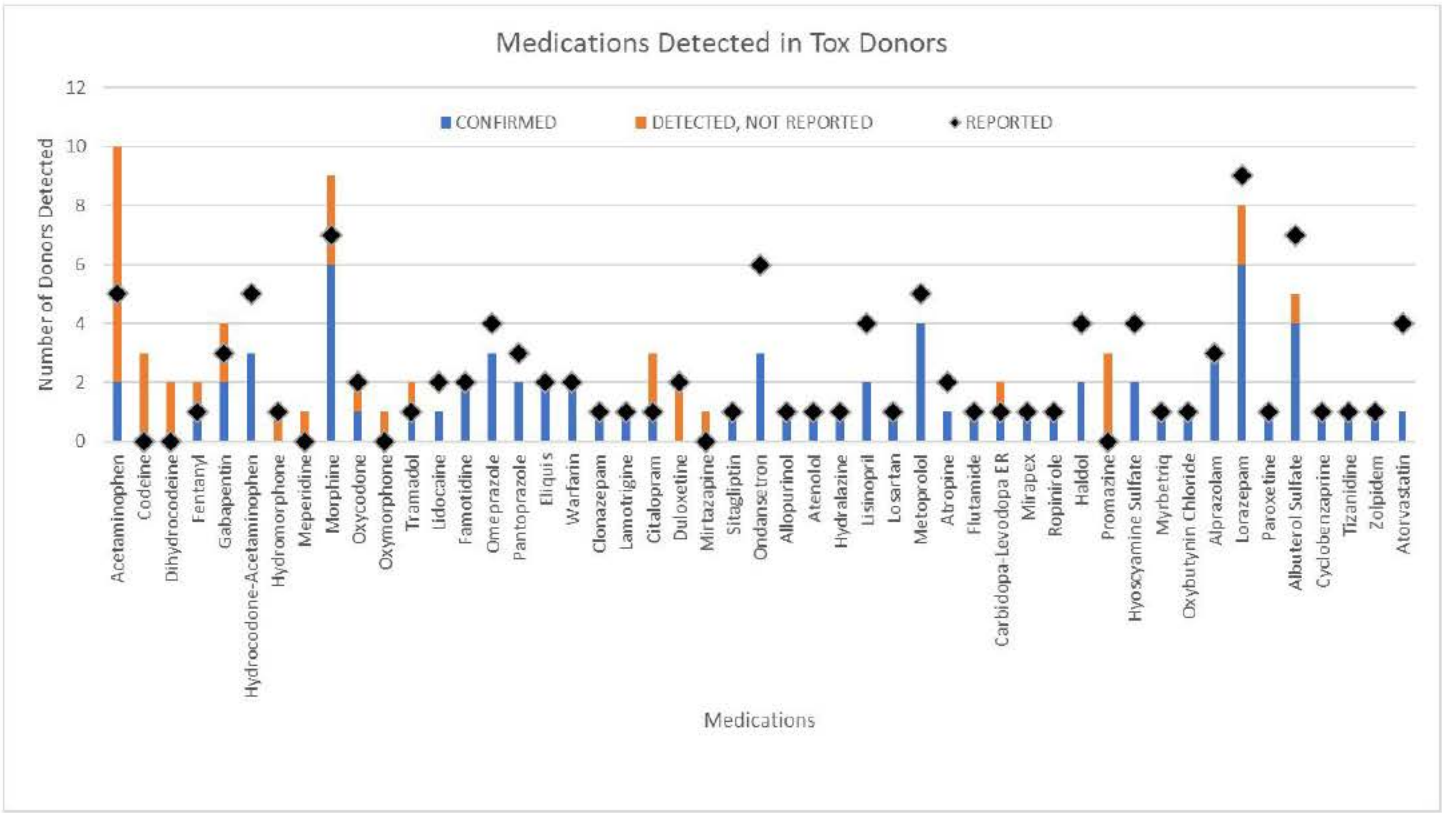

Figure 5. Toxicological screens of donors reveal approximately 54% of reported drugs were detected (blue) and 35% of drugs were found in sera or decomposition fluid but not reported (orange). The black diamonds represent the frequency of each drug reported.

Toxicological Screening Across Matrices

Toxicological screens of the non-serum matrices (decomposition fluid, larvae that fed on the body, and soil under the donor) demonstrated that metabolites detected in the serum were also found in the other matrices. In Figure 6, drugs and drug metabolites in green were both confirmed by the toxicological screens and were on the patient's medical history. Drugs shown in yellow were detected by our toxicological screens but not reported for the donor, and compounds in blue were measured from donors for whom we did not have a medication history. The intensity of the color indicates drug concentrations. The drugs had the highest concentrations in serum or decomposition fluid, although detectable amounts were also found in larvae and fluid-soaked soil.

Postmortem toxicology of Tox 019 exemplifies this trend of trackability for the analgesic morphine by demonstrating a defined route of the drug from the cadaver into the surrounding environment (Figure 7A). Not only was morphine present in the serum but also in larvae that were feeding on the cadaver and in decomposition fluid. Morphine was eventually detected in the CDI soil. Furthermore, the developmental stage of larvae seemed to influence drug detectability, with intensities of detectable drugs decreasing with older larval specimens.

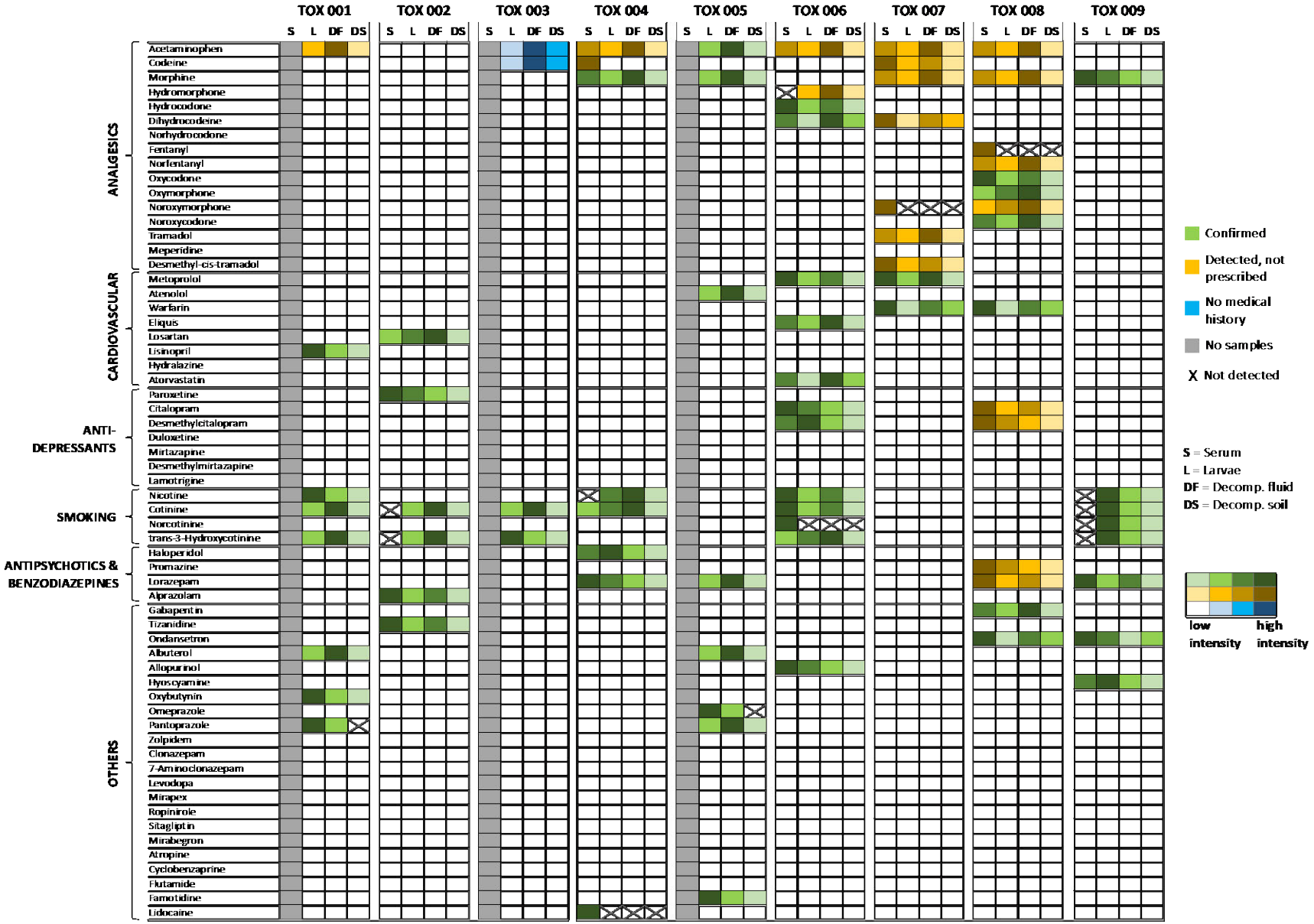

This resource was prepared by the author(s) using Federal funds provided by the U.S. Department of Justice. Opinions or points of view expressed are those of the author(s) and do not necessarily reflect the official position or policies of the U.S. Department of Justice.

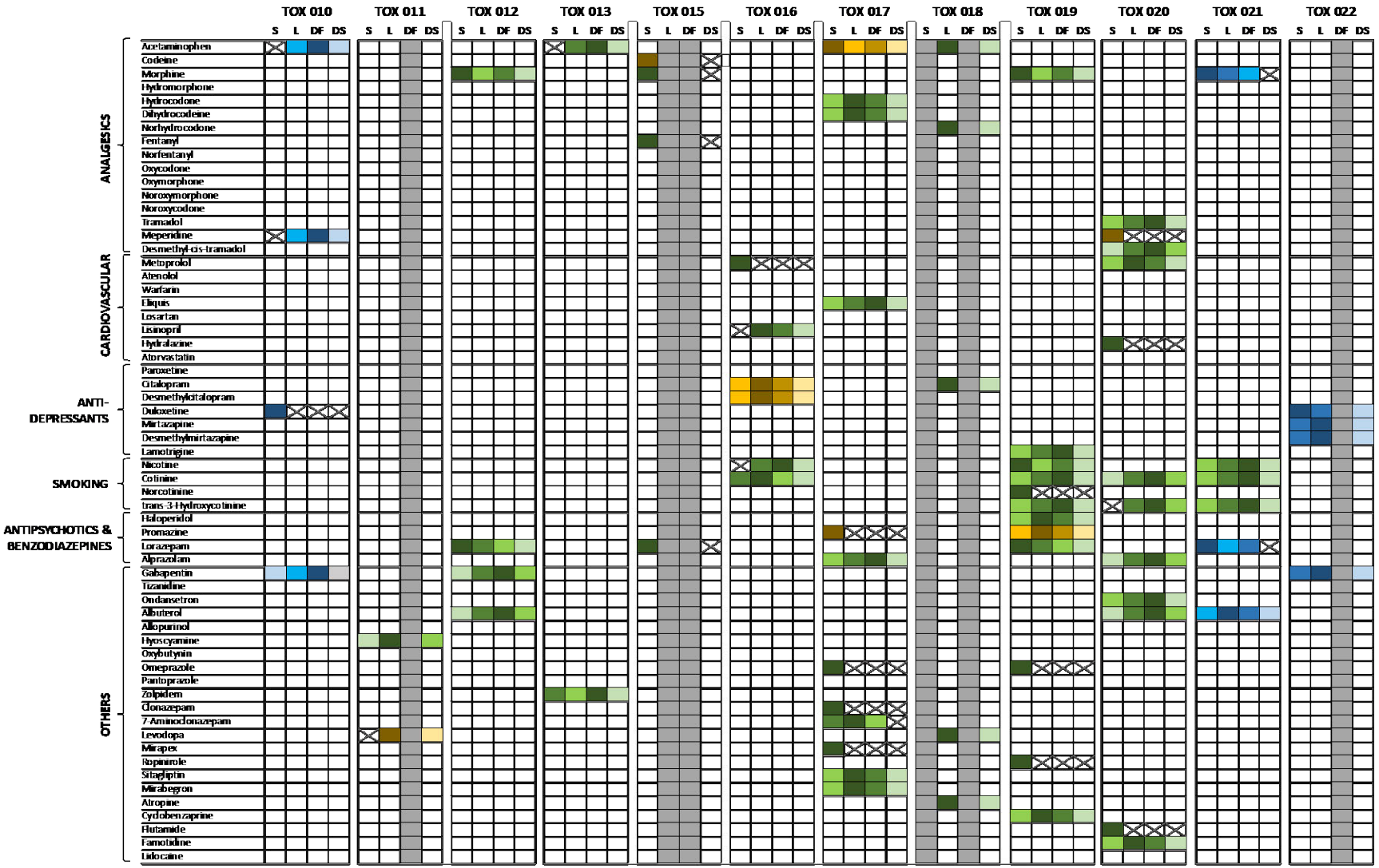

Figure 6. Toxicological screens of donors reveal that all donors had mixtures of drugs in their bodies (S), and during decomposition, these drugs are passed to larvae (L), decomposition fluids (DF) and soil (DS). Drugs and their metabolites were detected in all matrices from the 22 donors except in serum from donors Tox 001, 003, and 005 which we were unable to collect. Compounds in green (confirmed) were detected and were reported on the patient's medical history. Drugs in yellow were detected but not reported, and compounds in blue refer to donors for whom we do not have a medical history. The intensity of the color indicates relative drug concentration.

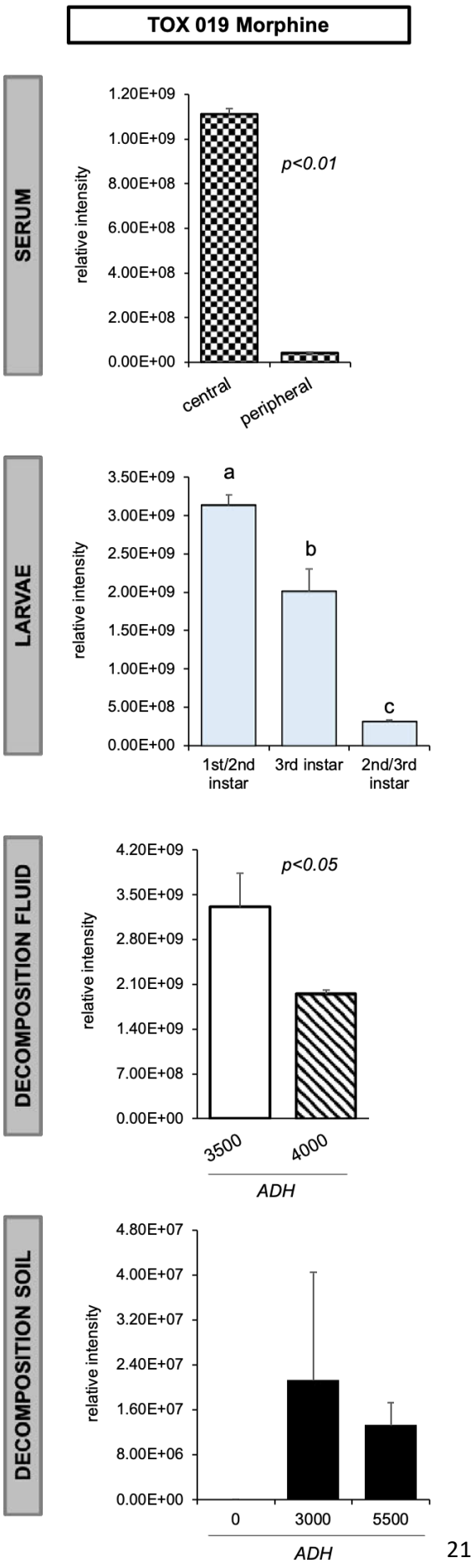

Figure 7. Toxicological analysis of different human postmortem matrices. Detection of morphine in the serum, larvae, fluid, and soil collected from donor Tox 019. Significant changes in drug abundances were derived using students t-test and one-way ANOVA. Letters are a result of post-hoc Tukey test.

This resource was prepared by the author(s) using Federal funds provided by the U.S. Department of Justice. Opinions or points of view expressed are those of the author(s) and do not necessarily reflect the official position or policies of the U.S. Department of Justice.

The sheer number of metabolites detected in our analyses provides a glimpse into the complexity and scale of metabolomic analyses with human serum and across the decomposer matrices, but also yields some potential biomarkers of human decomposition. We detected approximately 12,000 metabolites per sample in decomposition fluids and 3,000 in soils saturated with decomposition fluid adjacent to the donors. Decomposition increased the number of metabolites available to the microbial communities in the soil by more than 60%. Decomposition fluid, soil, and larvae from all 22 donors were extracted to analyze their metabolomes using PLS-DA. Overall, we noticed that the entirety of larvae, fluid, and soil samples collected from each donor had a specific metabolic signature that allowed discrimination amongst the donors (Figure 8A). For instance, larvae from Tox 002-004 seemed to be metabolically distinguishable from those collected from other donors, while decomposition fluid collected from Tox 010 showed a different metabolic profile and separated along the first component (72.3%). Analysis of decomposition soil revealed three distinct groups of donors exhibiting similar metabolomes. Intra-donor comparisons for soils (Figure 8B) showed increased metabolite abundances in decomposition soils compared to controls for later decomposition periods. As fluid is purged from the body during active decay, an accumulative influx of a diverse suite of metabolites can be expected in the soil. Further efforts were made to deconvolute time-dependent changes of the postmortem metabolome. Accordingly, data were split by percent ADH (0%, 25%, 50%, 75%, and 100% ADH) and analyzed using supervised, multivariate models (Figure 9A). Multiple donors (exemplified by Tox 005, 011, and 020) demonstrated a change in metabolic dynamics in the soil as decomposition progressed. Given the distinguishable cluster formation at each percent ADH interval, the metabolic composition of CDI soils appeared to shift over time. Samples forming 0% and 25% ADH clusters seemed to have distinct metabolic profiles (shown in yellow, Figure 9A) as they created a group separated from

the remaining three percent ADH classes (shown in blue, Figure 9A). Lastly, preliminary machine learning approaches identified several metabolites that could help to accurately classify a soil sample as decomposition or control soil. Specifically, our random forest classification algorithm predicted control and decomposition samples with 93% accuracy, identifying pantothenate, creatine, taurine, xylitol, xanthosine, and hypoxanthine as potential indicators of decomposition soils (Figure 9B). Generally, decomposing cadavers are a concentrated nutrient source affecting nitrogen, phosphorus, and carbon pools in the soil by providing a significant source of proteins and amino acids. Metabolites enriched in decomposition-impacted soils might have resulted from human global molecular mechanisms after death (e.g., breakdown of muscle tissue, nucleic acids) or via microbial-mediated processes – a topic that remains to be explicated in a future metabolome-microbiome analysis.

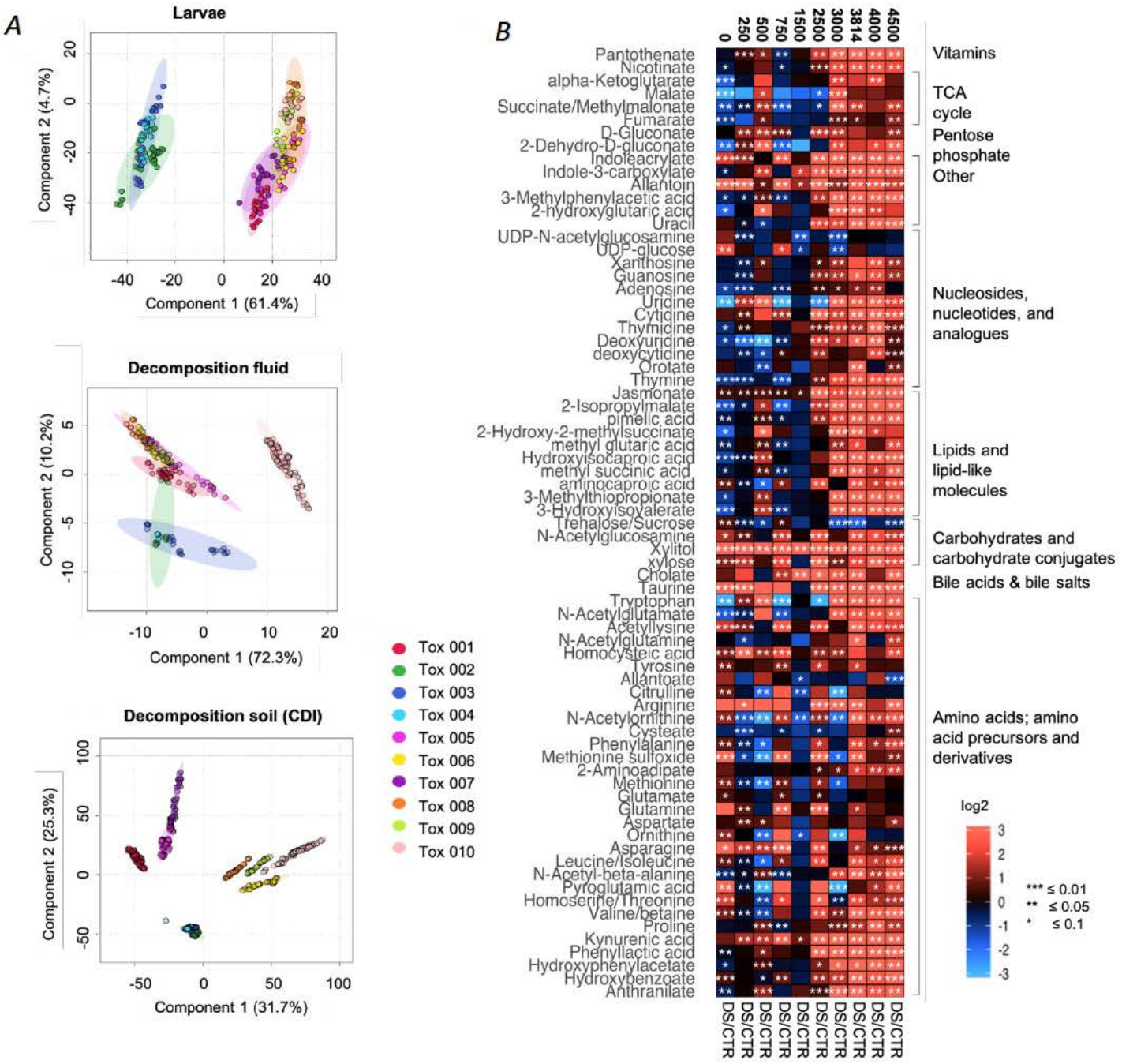

Figure 8. Postmortem metabolomics using UHPLC-HRMS. A) Partial least squares discriminant analysis (PLS-DA) of metabolomics data for larvae, decomposition fluid, and CDI soil. B) Intra-donor comparisons for Tox 009. Heatmap data are plotted as log2 transformed fold changes of decomposition soil (DS) to control soil (CTR) with an increase in relative metabolite concentrations shown in red, and a decrease in relative metabolite concentrations in blue. Time, measured in ADH, increases from left to right in the heatmap.

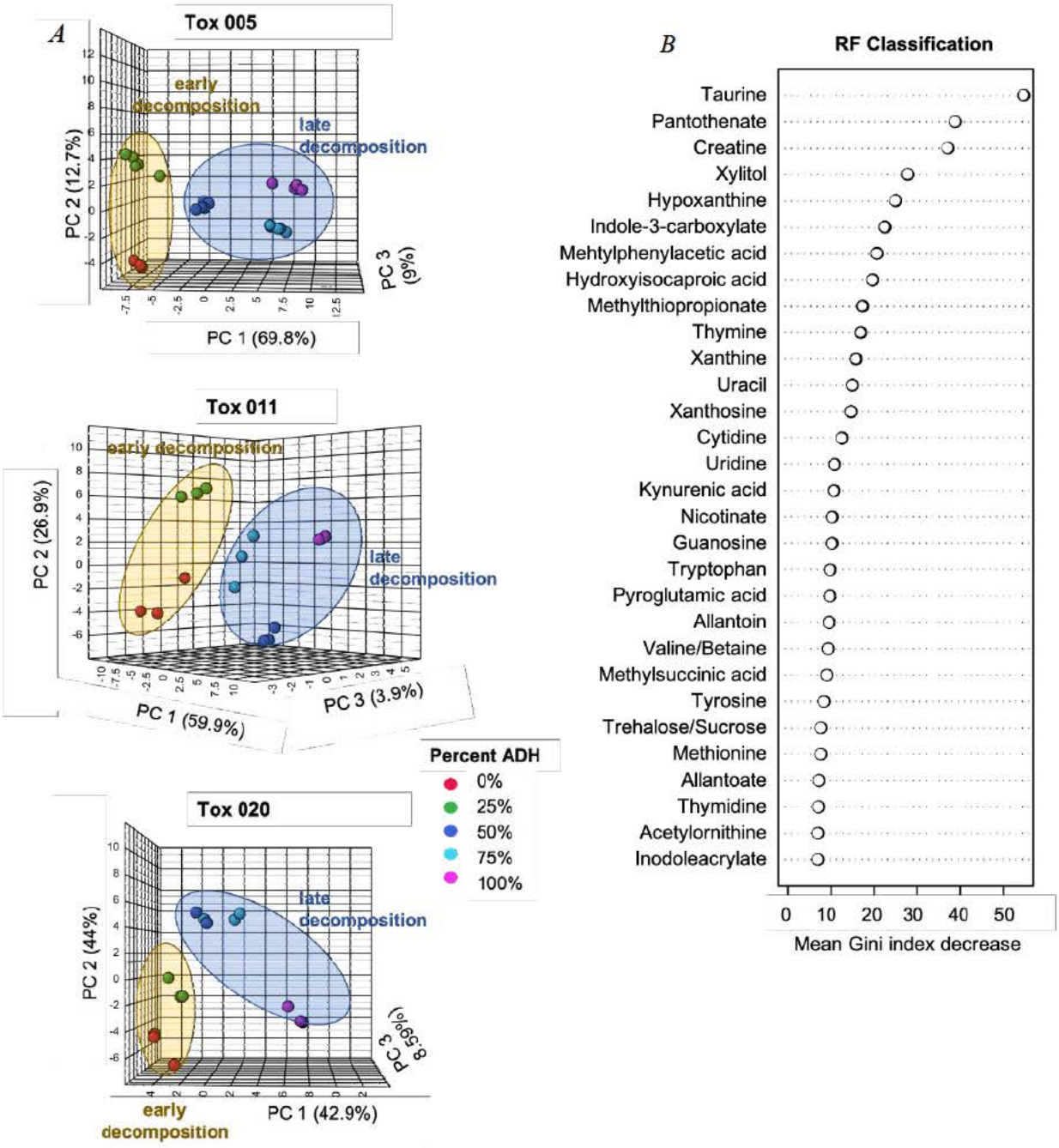

Figure 9. Postmortem metabolomics using UHPLC-HRMS. A) Metabolome changes over time in soils exemplified by Tox 005, Tox 011 and Tox 020. B) Preliminary random forest classification model on soil metabolomics data to discover soil decomposition biomarkers.

Decomposer Effects

Given that drugs enter the local environment, we are beginning to examine the effects of these drugs on the decomposers. Insect and microbial communities were impacted by both the reported medical conditions, especially cancer and diabetes, and by the drugs taken to treat these conditions. The scavenging data indicates raccoon preference for certain donors, though correlations with specific drugs or illnesses are not yet fully elucidated.

Soil Chemistry and Microbial Ecology

Soil chemistry analysis included electrical conductivity (EC), a measure of ionic strength in the soil, and pH, both of which can alter soil microbial activity. Soil responses between individuals were variable for both these parameters. EC in the soils within the cadaver decomposition island of all donors increased during active decomposition (Figure 10). This intensification was largely due to increases in ammonium from protein decomposition, though the rate and magnitude of this increase varied between donors. Tox donors 006, 012, 013, and 019 displayed the greatest increases in EC during active decomposition. We investigated if the presence of six end-of-life conditions (cancer, diabetes, cardiovascular diseases, neurological diseases, respiratory diseases, and pneumonia) impacted soil responses during decomposition. Of the six, only respiratory diseases displayed a trend, whereby individuals with respiratory diseases resulted in reduced EC increases over time compared to those without (Wilcoxon $p = 0.0009$). We also saw that season did not significantly impact EC increases over time (Kruskal $p = 0.85$).

The direction and magnitude of pH change within decomposition-impacted soils differed between individuals (Figure 10). Soils around the majority of donors ($n = 16$) decreased in soil pH during active decomposition, though soil pH increased around five donors. There was also a positive relationship between soil pH and leucine amino peptidase activity (LAP) response to

human decomposition (Figure 11), which may have implications for protein degradation patterns in decomposition soils, as LAP is an enzyme involved in protein degradation.

The effects of presence and absence of four disease categories (cancer, respiratory illnesses, cardiovascular illnesses, and neurological illnesses) and their influence on soil parameters over time were evaluated with hierarchical linear modeling (HLM). HLMs revealed that 1) pH decreased to a greater extent in decomposition soil of those with neurological illnesses compared to those without ($F = 30.79$; $p < 0.001$); 2) microbial respiration increased to a greater extent for those with cardiovascular illnesses over time ($F = 5.077$; $p = 0.026$); and 3) as ADH increased, individuals with cancer displayed a greater decrease in soil LAP activity ($F = 4.201$; $p = 0.045$) and reduced increase in microbial respiration ($F = 8.776$; $p = 0.004$). These preliminary trends do indicate that soil characteristics are influenced by donors with certain diseases and the complexity of interactions requires additional analysis.

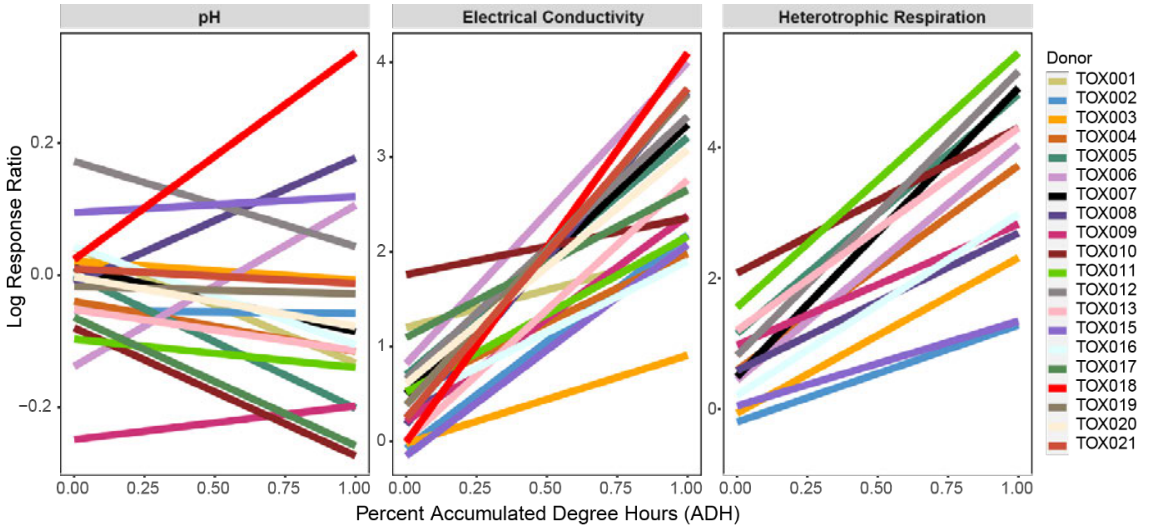

Figure 10. Soil parameter changes over time. Soil pH had variable response between donors, while electrical conductivity (EC), and heterotrophic respiration increased for all donors. Log response ratio (LRR) values (y-axis) are calculated by taking the natural log of the treatment value divided by the control value. Percent accumulated degree hours (x-axis) values were determined by dividing the ADH of the sample by final ADH of the donor, this allows for comparison of donors as the total time

This resource was prepared by the author(s) using Federal funds provided by the U.S. Department of Justice. Opinions or points of view expressed are those of the author(s) and do not necessarily reflect the official position or policies of the U.S. Department of Justice.

required to complete active decomposition varies between individuals. Linear regressions were used to generate trendlines and color corresponds to each donor and is consistent through all three panels.

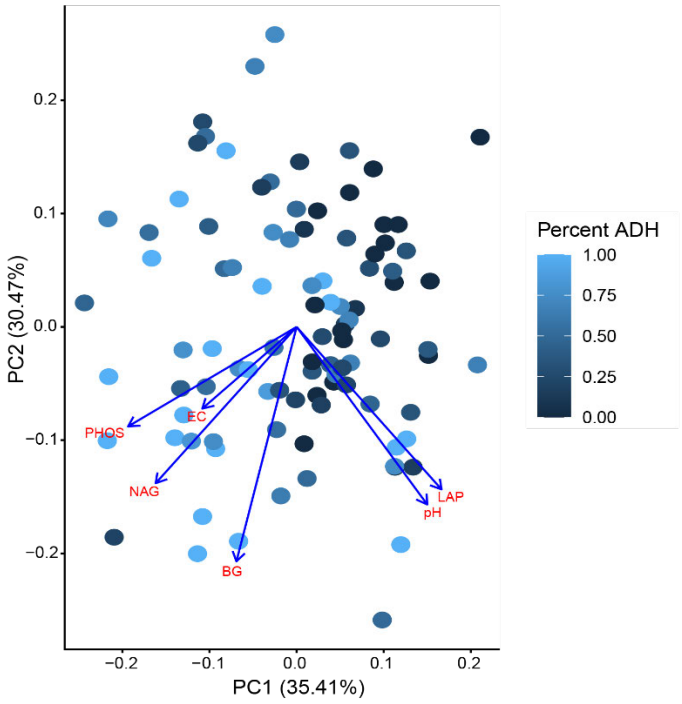

Figure 11. Principle components analysis (PCA) of soil chemical and enzyme profiles over active decomposition for Tox 011- 020. The log response ratio (calculated by taking the natural log of the treatment value divided by the control value) of the following soil parameters were used: pH, electrical conductivity (EC), and four enzyme activities (β-glucosidase, BG; N-acetyl-β-D-glucosaminidase, NAG; alkaline phosphatase, PHOS; leucine amino peptidase, LAP). Arrows represent the loadings of each variable, while color denotes time as percent of total ADH.

One of the key groups of decomposers are microbes: the bacteria and fungi in, on, and around the body that break down and metabolize dead tissues for their growth and energy, and whose communities change substantially during decomposition. Changes in microbial community structure were assessed using 16S rRNA gene (bacterial) and internal transcribed spacer (ITS) region (fungal) amplicon sequencing for donors Tox 001-020. In general, the richness (number of species) and diversity (richness plus distribution of the species) of soil microbial communities decreased during decomposition (Figure 12). However, inter-donor variability was observed, with

This resource was prepared by the author(s) using Federal funds provided by the U.S. Department of Justice. Opinions or points of view expressed are those of the author(s) and do not necessarily reflect the official position or policies of the U.S. Department of Justice.

some of these patterns correlating to medical conditions. For example, soil microbial communities under donors with neurological illnesses had a greater reduction in species richness (Figure 13C) (HLM, p = 0.026). Further, donors with cancer were associated with a slower increase in respiration rate (a metric of general activity; HLM, p = 0.004), and significantly reduced richness at ADH 4500 (Wilcoxon, p = 0.01) (Figure 13A). This suggests a strong disturbance and may be indicative of a toxic effect of cancer and neurological drugs on soil microbes. Conversely, microbial community richness decreased less under donors with respiratory illnesses (Figure 13 B, HLM, p = 0.035), suggesting drugs for respiratory illnesses may have a stimulatory effect on microbial diversity.

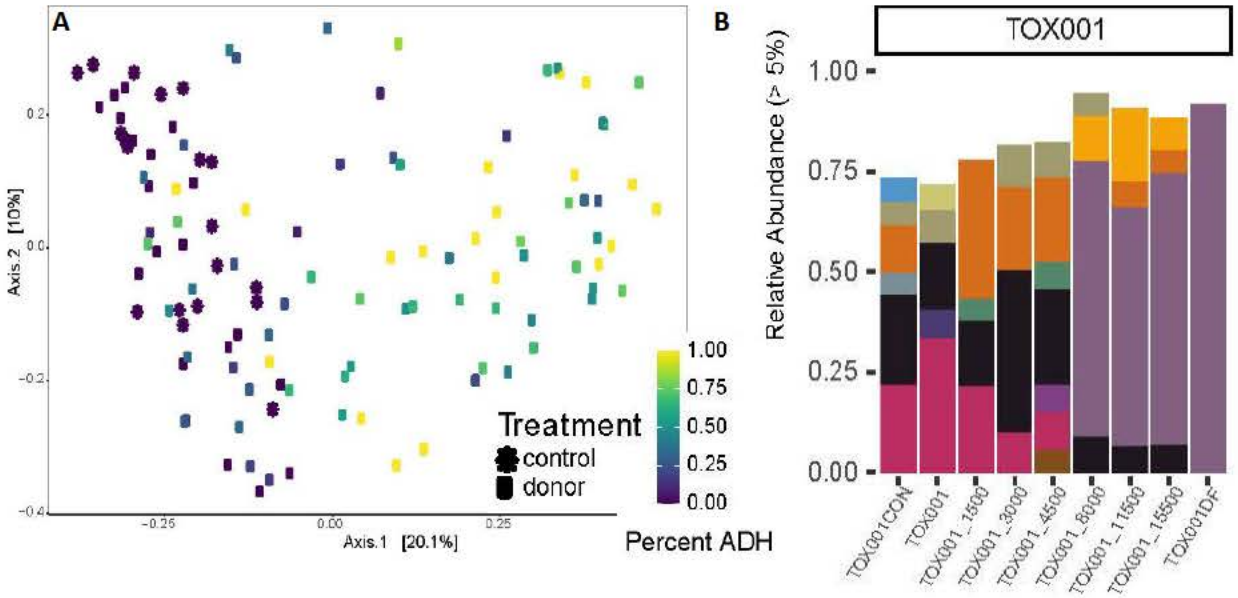

Figure 12. Change in fungal communities during human decomposition. A) PCOA of Bray-Curtis distances show communities change significantly as decomposition progresses (dark colors = early and controls; light colors = late) (n=20 donors). B) Saccharomycetes fungi was prevalent in the decomposition fluid (purple, far right bar), and increased in soil as decomposition progressed. Here, data from one donor (Tox001) is shown as an example.

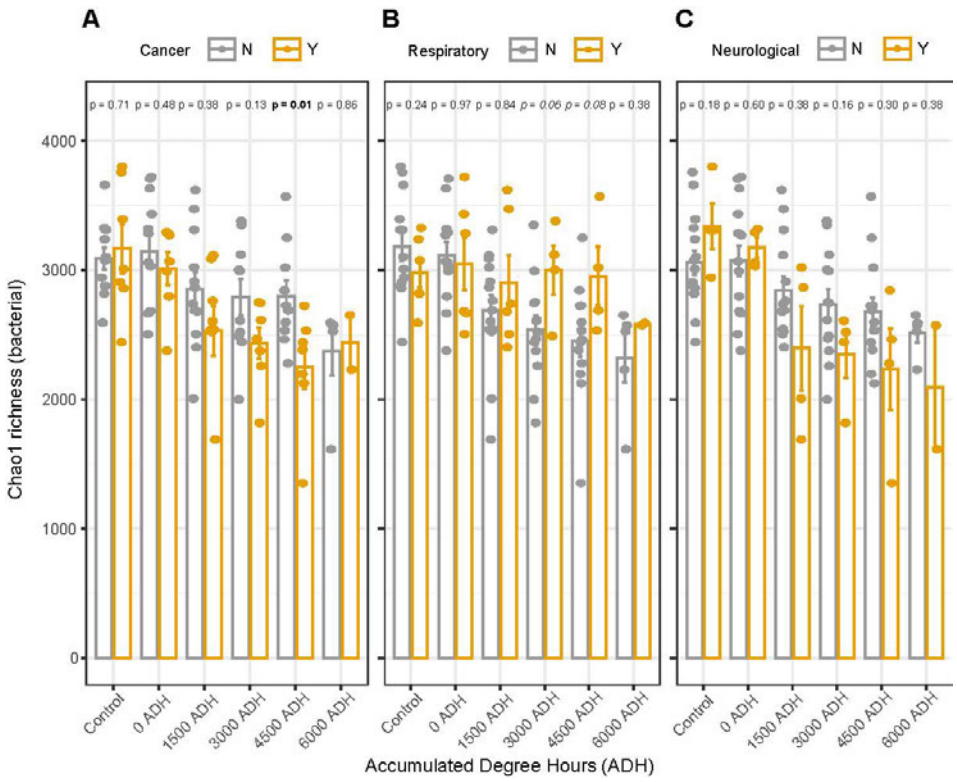

Figure 13. Species richness (Chao1 estimate) of soil microbial communities during decomposition is affected by donors with (gold) compared to those without (grey) cancer (A), respiratory (B) or neurological diseases (C). p values are from Wilcoxon tests between disease presence and absence at each time point (DeBruyn et al. in prep.)

Insect Activity

Adult female blow flies use chemoreceptors to assess suitability of carrion and determine the appropriate location to lay eggs. This behavior may be deterred by inopportune conditions and may delay colonization of a body. Therefore, we measured the pre-colonization interval (pre-CI) - the delay from donor placement to the first egg-laying event - to determine if drugs or disease condition impacted female fly oviposition. Pre-colonization intervals ranged from 2.8 – 2,760 h, or 54.5 – 5,664.9 ADH. The pre-CI was most strongly affected by seasons, with significantly longer pre-colonization intervals for donors placed in the winter compared to all other seasons ($P < 0.001$; Figure 14). No other drugs, disease conditions, or other biotic or abiotic factors significantly impacted the pre-CI in this preliminary analysis.

This resource was prepared by the author(s) using Federal funds provided by the U.S. Department of Justice. Opinions or points of view expressed are those of the author(s) and do not necessarily reflect the official position or policies of the U.S. Department of Justice.

Species richness (S) and Simpson diversity (D) were highly variable among donors and overall beta diversity was moderately high among donors ($\beta = 0.502$). Eleven blow fly species were collected during this project. The most common and abundant larval and adult species was *Phormia regina*, as it was collected from 19 out of 22 donors. Included in this highly diverse sample is *Chrysomya megacephala* (Fabricius), which represents a new distribution record for this species in the state of Tennessee (Owings et al. 2021). Donor Tox 021 exhibited the greatest larval blow fly richness compared to the other donors (five species compared to a mean of 1.85 for all other donors) (Figure 14 B,C). Tox 022 exhibited the highest adult blow fly richness, with six species compared to a mean of 1.38 species for all other donors. While this diversity may be due to the extended period in active decomposition, it is also notable that this was the only donor to have a combination of anti-psychotic and anti-depressant drugs detected in the serum. Season was the biggest predictor of changes in species richness, with the most species detected in the fall, and the fewest species detected in the summer (Figure 14B). No drugs, disease conditions, intrinsic, or other extrinsic variables significantly impacted larval richness of donors in this study.

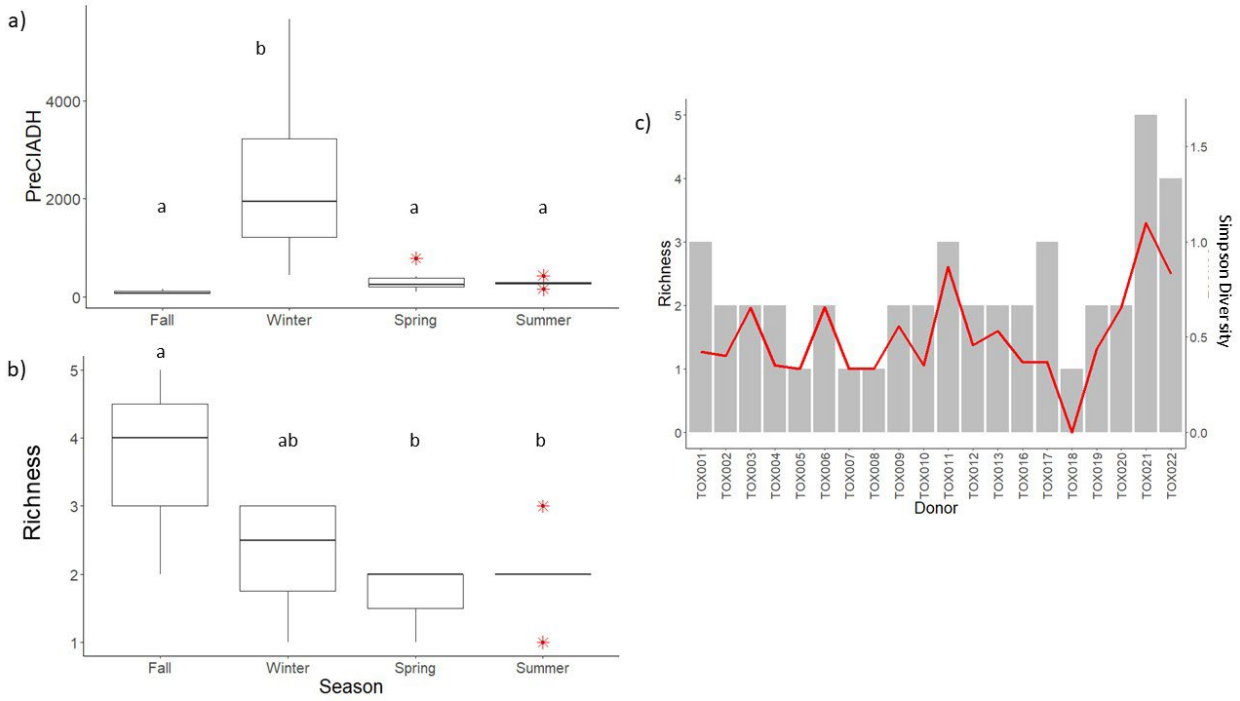

Figure 14. A) Pre-CI in different seasons, B) richness in different seasons, and C) the richness and diversity over donor.

The larval length of *Phormia regina* was analyzed from the 12 donors colonized by this species. A strong seasonal effect was observed, with significantly shorter larvae collected in the winter compared to all other seasons ($P < 0.05$ for all comparisons). Inter-donor variability was also significant ($P = 0.000$) and a Wilcoxon test was implemented to obtain pairwise comparisons (Table 3). Notably, Tox 021 exhibited significantly shorter larvae compared to all donors except Tox 020 ($P = 0.000$), and Tox 022 exhibited significantly longer larvae compared to all donors except Tox 003, Tox 011, and Tox 020 ($P = 0.000$). Though both Tox 021 and 022 were placed in the fall within a few weeks of each other, temperatures were still warm for most of Tox 021's decomposition, whereas temperatures began cooling down after Tox 022 was placed. This difference in temperature could explain the drastic larval size difference from these donors, but further statistical analyses will need to be implemented to explain these differences. However, it is notable that Tox 021 had tobacco-related drugs as well as an opioid in the blood serum, whereas

This resource was prepared by the author(s) using Federal funds provided by the U.S. Department of Justice. Opinions or points of view expressed are those of the author(s) and do not necessarily reflect the official position or policies of the U.S. Department of Justice.

Tox 022 had anti-depressants. Additionally, donors with antemortem cancer or diabetes diagnoses exhibited significantly longer larvae compared to donors without these conditions (P = 0.006, 0.000 respectively). Intrinsic conditions associated with these antemortem diseases may have acted to extend the larval developmental duration on each donor, leading to an overall increase in body size. Conversely, donors with antemortem cardiovascular conditions exhibited significantly shorter larvae compared to those without such conditions (P = 0.000), which indicates that such a disease may increase the rate of larval development, thus decreasing overall body size.

Table 2. Summary of a statistically significant (at P=005) pairwise comparisons of larval length resulting from a Wilcoxon test.

Donor A	Donor B	*P* value
Tox 002	Tox 004	0.047
Tox 017	Tox 002, Tox 003, Tox 021, Tox 022	<0.001
Tox 021	All donors except Tox 020	<0.001
Tox 022	All donors except Tox 003, Tox 011, and Tox 020	<0.001

Though there were several significant results in our analysis of larval length, it is important to note that numerous abiotic and biotic factors can contribute to development rate and body size differences in insects. These include temperature (Byrd and Allen 2001), density (Goodbrod and Goff 1990), predation (Wells and Greenberg 1992), competition (Wells and Greenberg 1994), non-consumptive effects (Flores et al. 2017), phenotypic plasticity (Gallagher et al. 2010, Owings et al. 2014), population genetics (Picard and Wells 2009, 2010), and sex (Picard et al. 2013), to name a few. Therefore, there may be numerous environmental and ecological factors contributing to growth and development of larvae on human and animal remains that were not accounted for in this analysis. Some of these factors will be taken into account in future statistical analysis (e.g., temperature, competition), though others (e.g., genomic analyses of larvae) will need to be investigated in future studies.

Scavengers

Scavenger preference may also be affected by drugs in the body, as evidenced by differential scavenging among the 22 donors. The primary scavenger observed throughout the duration of the project was the common raccoon (*Procyon lotor*). Tox 013 can be considered a "control" for these purposes as this donor died of suicide rather than chronic disease, only reported taking three drugs (Ambien, Imitrex, Sildenafil), and only Ambien was detected in their system. No scavenging of this donor occurred at all. Another case example is Tox 001, who had a long list of medications related to heart disease and who died of coronary artery disease, hypertension and diabetes. Raccoons visited the body frequently, but the minimum number of scavenging events (MNSS) were relatively low compared to the number of visits, suggesting the body was not particularly attractive for consumption. In contrast, Tox 006 was completely scavenged throughout the body (Figure 15), not only by raccoons but also by an opossum and a cat. This donor died from lymphoma, COPD and renal failure, and was prescribed a number of analgesics, including opioids, related to chronic disease suffering. Moreover, the timeframe of enrollment of Tox 001 and Tox 006 at the ARF overlapped, indicating that the scavengers had equal access to both donors simultaneously but made specific choices. Though this current sample size is too small for statistically significant relationships, Tox 006 exemplifies an observed trend towards greater scavenging activity on donors with nicotine and/or opioid use. Seasonal or temperature variation does not explain differential scavenging. The variation in scavenging observed shows that raccoons (and perhaps other scavengers) have preferences for human tissue consumption that may be related to end of life disease and/or drugs in the system.

Figure 15. Comparison of scavenging activity of Tox 001 (left) on the last day of enrollment (Day 93) who was not scavenged, to Tox 006 (right) also on the last date of enrollment (Day 17) whose arm bones and cranium are fully exposed and diarticulated and leg muscles consumed by scavengers.

Impact on Decomposition Rates and Postmortem Interval

Given that we have documented that drugs can be detected across decomposer matrices, we hypothesized that inter-donor variation in microbe, soil chemistry and insect diversity may affect postmortem interval (PMI) estimates. While preliminary trends are provided here, additional computational analyses are forthcoming that will better model the effects of both intrinsic (disease, drug metabolites, BMI) and extrinsic variables (particularly seasonality) on PMI.

As demonstrated in Table 5, there are differences in the length of time an individual takes to complete active decomposition even within seasons. For instance, donors placed at the ARF in the summer months completed active decomposition in as little as 4934 ADH (Tox 009), but also took as long as 17460 ADH (Tox 010). Fall and winter had the most variability in decomposition time

(4113-46398 ADH when placed in the Fall and 6005-18460 ADH for winter placements). This indicates that season alone does not explain decomposition variability. Figure 18 demonstrates that medical conditions could partly explain the length of time required to complete active decomposition; specifically, those with cardiovascular illness, pneumonia and diabetes were slower to decompose than those without these diseases. Additional experiments are needed to fully understand the mechanism behind these trends, but a brief overview of microbial ecology and larval development may provide some insight.

Table 3. Dates of placement and unenrollment at the end of active decay, with total number of days observed and final ADH and ADD for each donor.

Research Number	Date of Placement (D, M,Y)	Date Removed From Study	Days Observed	Known ADH	Known ADD	Season of Placement
TOX002	13 Mar 19	15 Apr 19	34	3845	165	Spring
TOX003	2 Apr 19	29 Apr 19	28	4578	207	Spring
TOX004	23 Apr 19	8 May 19	16	3556	153	Spring
TOX005	26 Apr 19	29 May 19	34	8631	380	Spring
TOX006	13 May 19	29 May 19	17	4391	230	Spring
TOX007	16 May 19	3 June 19	19	6099	264	Spring
TOX008	10 June 19	2 July 19	22	6813	295	Summer
TOX009	24 June 19	8 July 19	14	4934	225	Summer
TOX010	9 July 19	28 Aug 19	50	17460	755	Summer
TOX011	31 July 19	20 Aug 19	22	7238	318	Summer
TOX012	20 Sep 19	7 Oct 19	17	6046	276	Summer
TOX013	20 Sep 19	15 Oct 19	25	7490	338	Summer
TOX021	8 Sep 20	13 Oct 20	35	7561	342	Summer
TOX014	24 Sep 19	5 Oct 19	11	4113	184	Fall
TOX015	22 Oct 19	18 Nov 19	27	1423	50	Fall
TOX016	4 Nov 19	30 Dec 19	57	1531	47	Fall
TOX022	2 Oct 20	13 Aug 21	315	46398	1948	Fall
TOX001	25 Feb 19	29 May 19	93	16225	684	Winter
TOX017	4 Dec 19	12 Jun 20	191	18460	789	Winter
TOX018	10 Jan 20	24 Mar 20	74	4027	168	Winter
TOX019	28 Jan 20	9 Apr 20	72	5607	218	Winter
TOX020	11 Mar 20	28 Apr 20	48	6005	251	Winter

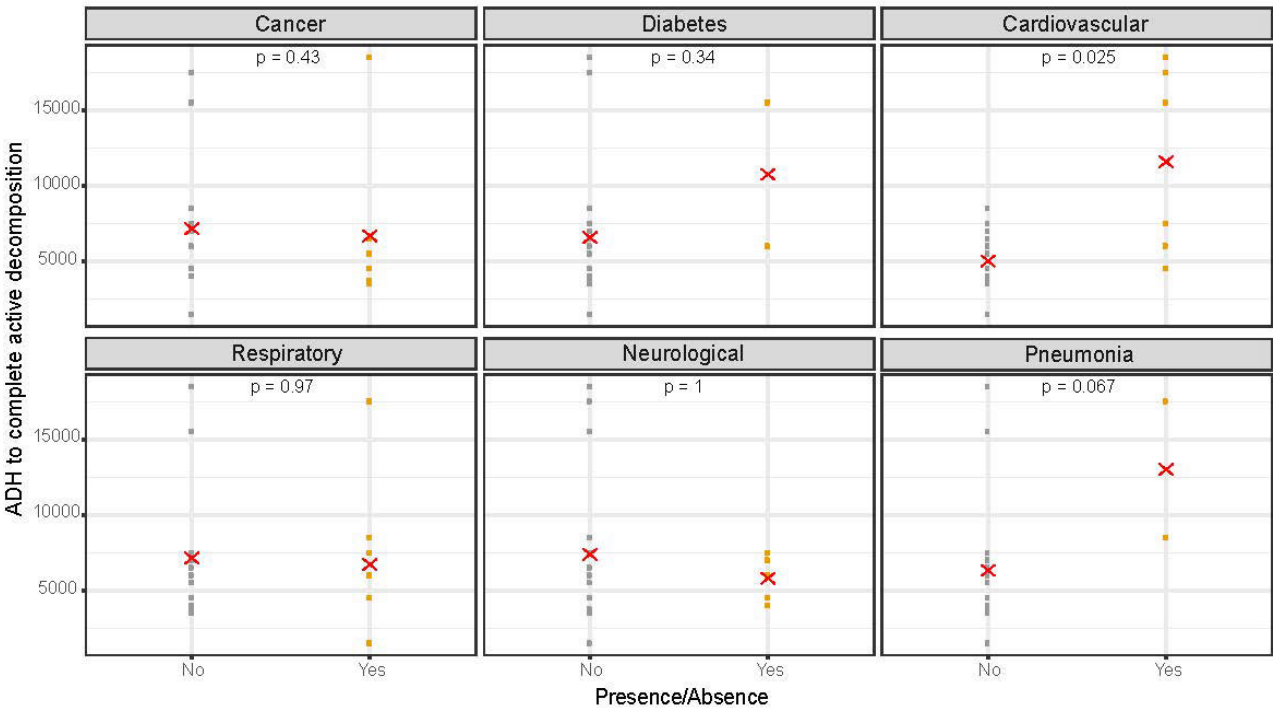

Figure 16. Comparison of the total ADH required to complete active decomposition between donors with (yellow) and without (grey) different illnesses. Panel A – cancer, B – diabetes, C- cardiovascular, D – respiratory, E- neurological, F- pneumonia. Red x's indicate group means and p-values were derived from Wilcoxon tests.

Microbial Ecology

To date, the use of a "microbial clock" to estimate PMI has not been validated in human remains (though see Deel et al. 2020; Metcalf et al. 2013; Pechal et al. 2013) so we did not employ a specific method to evaluate PMI, but rather examined microbial community composition and diversity. Soil microbial community composition (bacterial and fungal) clearly changed during active decomposition (Figure 17), however differences between the bacterial and fungal community responses were observed. While fungal community composition becomes more similar as decomposition progresses (Figure 17B), bacterial communities were more variable from the onset and did not become more similar (Figure 17A). Statistical beta dispersion (a measure of variability between donors over time) shows that dispersion within soil bacterial communities

varied between individuals (Figure 18A; F=3.5277; p=0.001). In contrast, dispersion within soil fungal communities does not differ between individuals (Figure 18B; F=0.7168; p=0.789). These data show that decomposition disturbs soil microbial communities, but that the changes in soil bacterial communities are not consistent between individuals.

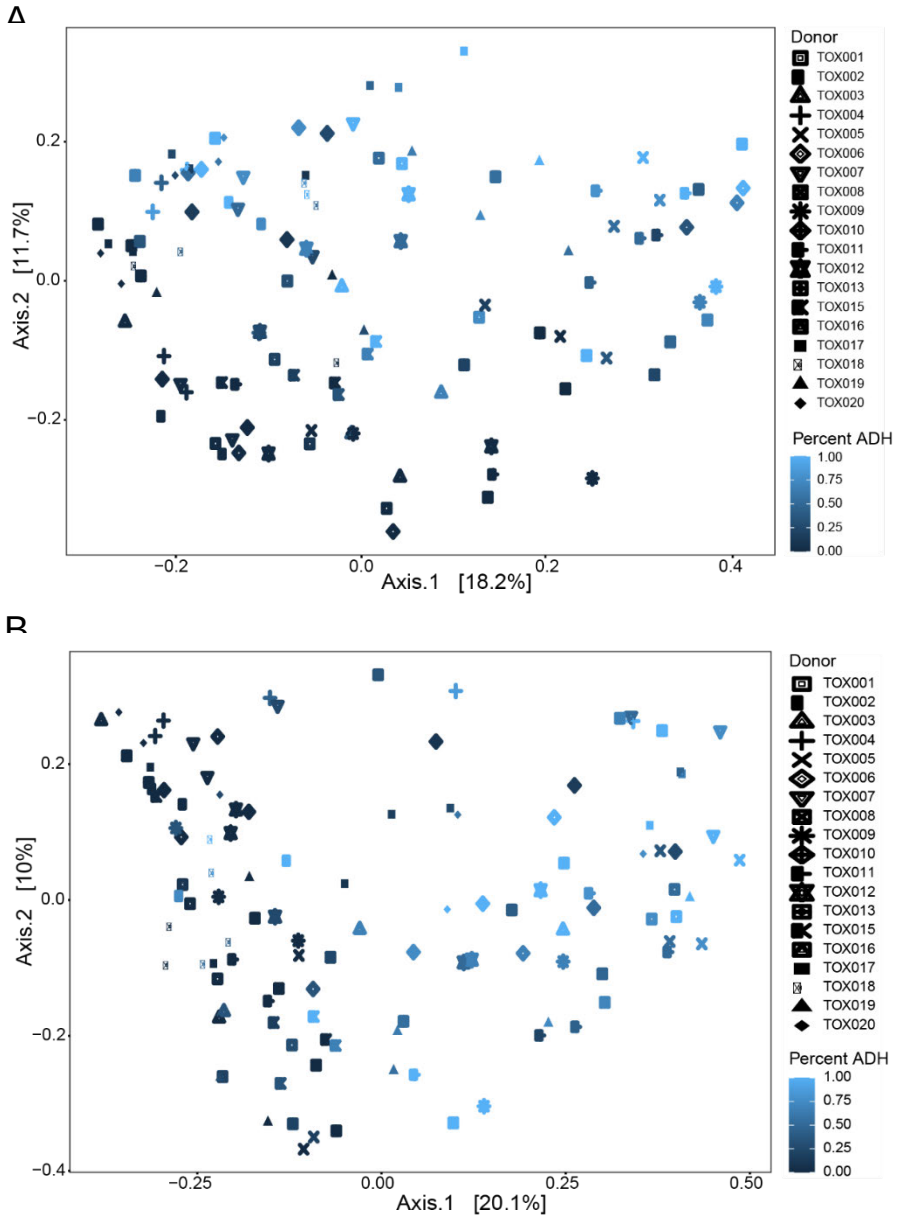

Figure 17. Bray-Curtis distance-based principal coordinate analysis (PCoA) of soil bacterial (A) and fungal (B) communities for Tox 001-020 show compositional shifts during active decomposition. Symbols denote donor, while color represents time in percent ADH.

This resource was prepared by the author(s) using Federal funds provided by the U.S. Department of Justice. Opinions or points of view expressed are those of the author(s) and do not necessarily reflect the official position or policies of the U.S. Department of Justice.

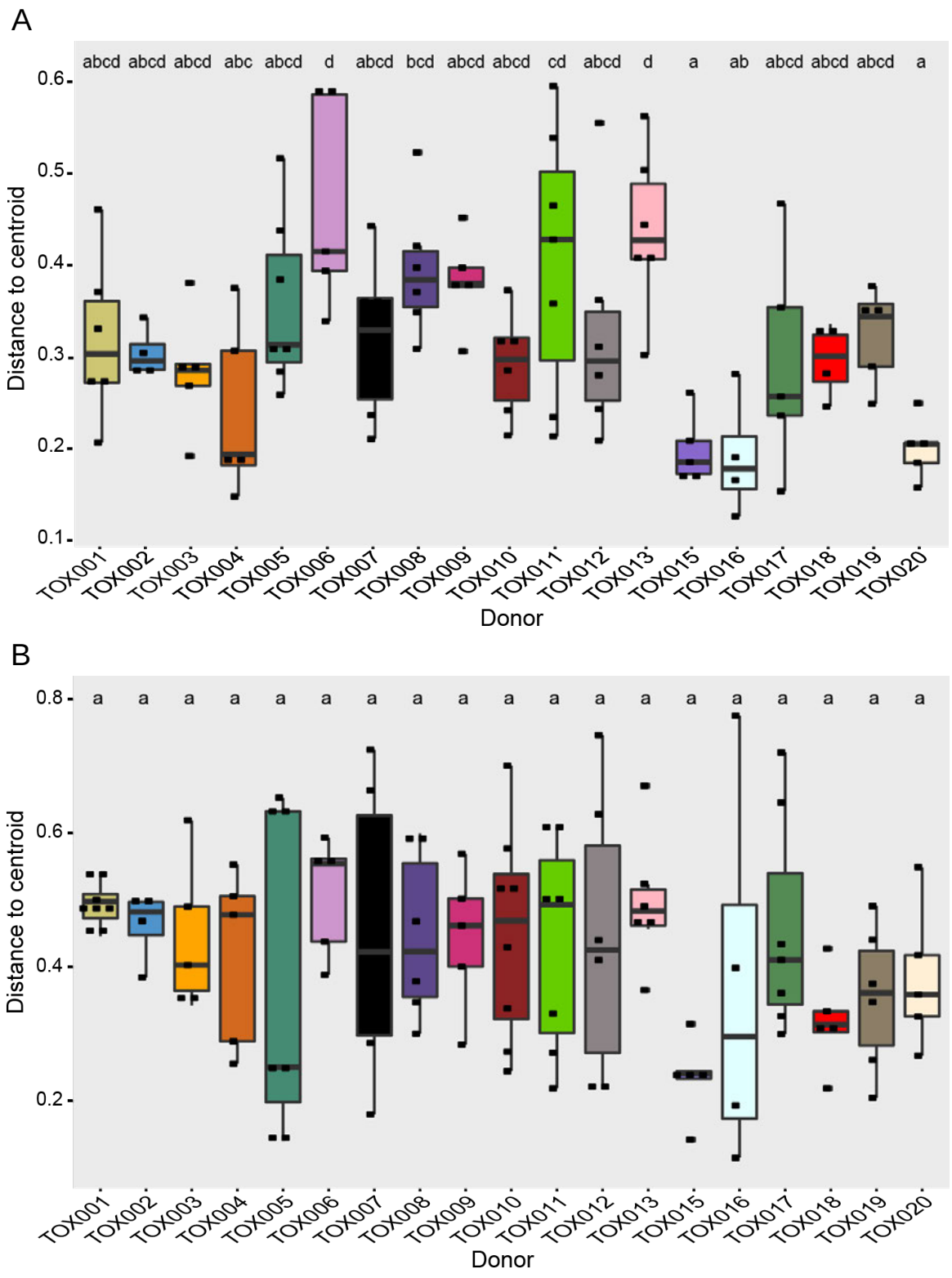

Figure 18. Statistical beta dispersion (y-axis) of soil bacterial (A) and fungal (B) communities between individuals (x-axis). Color represents individual, while letters at the top of each figure are the result of post-hoc Tukey tests. Dispersion of bacterial communities varies between individual, while fungal communities do not.

This resource was prepared by the author(s) using Federal funds provided by the U.S. Department of Justice. Opinions or points of view expressed are those of the author(s) and do not necessarily reflect the official position or policies of the U.S. Department of Justice.

Entomological Methods of PMI Estimation

Larval age estimations are the most accurate method in forensic entomology to determine the time of colonization (TOC), or when the specimens in question began their life cycle on the body. The TOC is then used to infer a portion of the PMI. In order to make this type of estimation, the development stage (e.g., egg, 1st instar, 2nd instar, 3rd instar, post-feeding 3rd instar, or pupa) is determined, and then a species identification is made. Once the species and stage are known, previously published developmental datasets are used to determine the length of time required to reach the respective stage under conditions similar to those experienced by larvae at the death scene. Once the development time is known, it is transformed to accumulated degree hours and used to go back in time from the point at which larval samples were collected from the body. This estimated window of time comprises the TOC. In this analysis, an estimation was considered accurate if it fell within the minimum and maximum estimated range for a given species.

Overall, 352 TOC estimations were generated for all larval blow fly species sampled throughout decomposition for each of the 22 donors. Using samples from all timepoints throughout decomposition revealed an accuracy of only 31%, with 50% of estimations underestimating the time of donor placement, and 19% overestimating the time of placement. Since entomological estimations are based on the development of insects with only an approximate two-week life cycle, larval samples taken after this time period usually result in underestimations of the TOC. Therefore, in order to account for this biological timeline and to glean more insight about the utility of certain colonizers, only estimations made at or earlier than 3000 ADH for each donor were used for further analysis (N = 157 estimations). Using this updated dataset, 61% of all estimations were accurate, with underestimations accounting for 11% and overestimations accounting for 28% of inaccuracies. When TOC accuracy was assessed by drug class, there were no significant

interactions detected (Figure 19). No other abiotic factors were found to be significant in predicting TOC estimation accuracy. However, the species of blow fly used to make an estimation was significant for TOC accuracy ($P < 0.001$). While this preliminary analysis does not indicate that drugs impacted entomological PMI estimation, the fact remains that insect physiology has been shown to be significantly impacted by human-derived drugs, including those found in our donor populations, such as opioids (e.g., George et al. 2009). Additional field and directed laboratory experiments will better elucidate the impact of drugs on entomological PMI estimations.

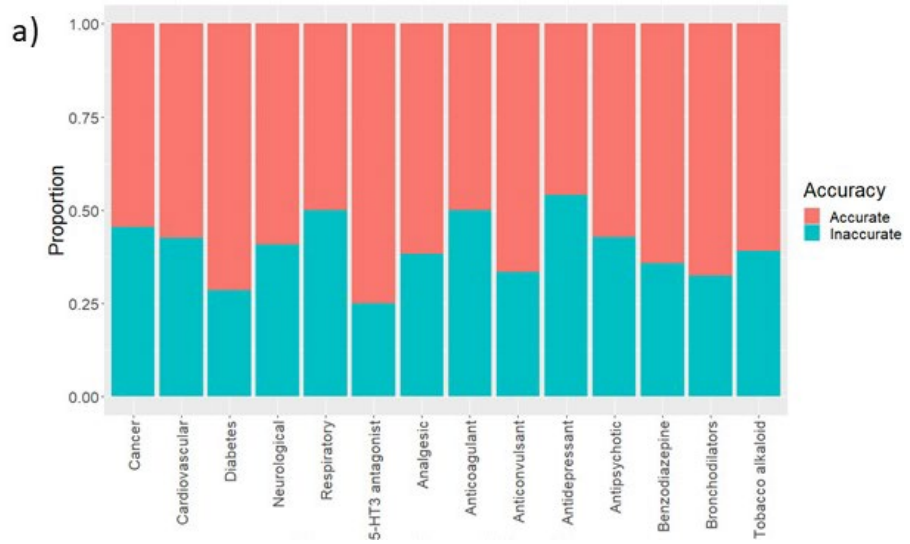

Figure 19. 100% stacked bar graph illustrating the time of colonization accuracy by drug class, where coral represents accurate estimations and teal represents inaccurate estimations.

Morphological PMI Methods – Total Body Score

Megyesi et al. (2005) developed the Total Body Score (TBS) as a means to correlate the morphological changes of decomposition with time since death, measured in ADD. Table 6 provides the estimated ADD and known ADD for each donor, as measured from placement until unenrollment (end of active decomposition). The estimated ADD range is calculated using the point estimate and the standard error (±388.16). The estimated ADD derived from the TBS equation is considered accurate if the known ADD falls within the error range. Given that this

This resource was prepared by the author(s) using Federal funds provided by the U.S. Department of Justice. Opinions or points of view expressed are those of the author(s) and do not necessarily reflect the official position or policies of the U.S. Department of Justice.

range is quite large (covering 776 ADD), only 32% of known ADDs fell outside of the estimated range. The estimated ADD underestimated the known ADD for three donors (Tox 001, 018 and 022) and overestimated the known ADD for four other donors (Tox 006, 015, 016 and 021). The TBS method does not account for insect activity or scavenger-related changes (e.g., early bone exposure due to raccoon damage) which may artificially elevate the estimated ADDs. This is evidenced by Tox 006 whose ADD was overestimated by almost 1000 ADD, but was also heavily scavenged. Preliminary analysis indicates there is no statistically significant correlation between end-of-life condition and/or toxicology and the accuracy of TBS, though more complex models are required to tease apart seasonal and intrinsic effects and metabolic covariates expressed among these individuals.

Table 4. Estimated and known ADD for each donor. Blue text – TBS estimated ADD underestimated known ADD; Red text – TBS estimated ADD overestimated known ADD.

Donor	Est. ADD from TBS	Est. ADD Range*	Known ADD	Season
TOX001	494.7314	106.5714-882.8914	684	Winter
TOX018	167.9046	0-556.0646	168	Winter
TOX022	710.8439	322.6839-1099.0039	1948	Fall
TOX006	1228.658	840.498-1616.818	230	Spring
TOX015	1080.176	692.016-1468.336	50	Fall
TOX016	527.7409	139.5809-915.9009	47	Fall
TOX021	916.2205	528.0605-1304.3805	342	Summer
TOX002	559.3678	171.2078-947.5278	165	Spring
TOX003	313.0589	0-701.2189	207	Spring
TOX004	704.13	315.97-1092.29	153	Spring
TOX005	609.9116	221.7516-998.0716	380	Spring
TOX007	480.6816	92.5216-868.8416	264	Spring
TOX008	390.9521	2.7921-778.681	295	Summer
TOX009	557.2263	169.0663-945.3863	225	Summer
TOX010	953.5677	565.4077-1341.7277	755	Summer
TOX011	362.4306	0-750.5906	318	Summer
TOX012	279.0416	0-667.2016	276	Summer
TOX013	269.9848	0-658.1448	338	Summer
TOX014	333.1358	0-721.2958	184	Fall

TOX017	181.97	0-570.13	789	Winter
TOX019	156.9228	0-545.0828	218	Winter
TOX020	244.3431	0-632.5031	251	Winter

*The range is calculated using the standard error of the ADD estimate, ±388.16 (Megyesi et al. 2005).

Conclusions

Our study is the first to provide systematic data on how donors with known multi-drug loading directly impact their decomposers. Our research demonstrates that parent drugs and their metabolites can be traced from a decomposing body to its decomposers, and we are beginning to understand the effects those drugs have on each biosystem studied. Our analyses found thousands of drug-related metabolites among 22 donors that transferred to decomposer matrices, and some of these metabolites may become important biomarkers of decomposition. The results show inter-donor variability based on intrinsic factors exists, highlighting a need to further investigate the effects of intrinsic traits on decomposition processes and incorporate these findings into PMI estimates. For instance, analyses reveal significant variation in both the arthropod assemblage and the developmental trajectory of larvae among donors, likely caused by toxicological loading and environmental factors unique to certain species. Trends of donors with drugs related to specific disease classes also caused quantifiable inter-donor shifts among soil microbe communities. When taken together, these analyses indicate that the antemortem activities of donors have significant impacts on their own decomposition processes as well as the biology and ecology of the organisms that colonize or scavenge them after death.

Deliverables

Deliverables completed to date include the materials below as well as semi-annual reports. In addition, we anticipate a minimum of four additional publications and another dissertation that

will disseminate the methods and results of our work. All metabolomics data will also be made available through the MetaboLights database concurrent with manuscript submission.

Publications

Owings, Charity G., Hayden S. McKee-Zech, Dawnie W. Steadman. 2021. First record of the Oriental Latrine Fly *Chrysomya megacephala* (Fabricius) (Diptera: Calliphoridae) in Tennessee, USA. *Acta Parasitologica*, 1 – 3.

Owings, Charity G., Megan S. McQueen, Mary E. Smith, Riley K. Wal, Hayden S. Mckee-Zech. 2021. Rearing container size impacts immature development time of *Phormia regina* (Meigen) (Diptera: Calliphoridae) and time of colonization estimations. *Journal of Forensic Entomology*. (in press)

Presented Papers

Owings C.G., McKee-Zech H., Patrick E., Schwing S., Delgado T., Steadman D.W. (2022) Pre-colonization data improves larval age estimations with human remains. Abstract accepted as an oral presentation for the 2022 Academy of Forensic Sciences annual meeting (Seattle, WA). February 24, 2022.

Mason A.R., McKee-Zech H.S, Höland K., Schwing S., Patrick E., Campagna S., Steadman D.W., DeBruyn J. (2022) Tuning microbial succession-based postmortem interval (PMI) estimation models: The effect of environmental parameters on model prediction. Abstract accepted as a poster presentation for the 2022 Academy of Forensic Sciences annual meeting (Seattle, WA). February 24, 2022.

Mason A.R., McKee-Zech H.S., Höland K.M., May A., Davis M.C., Schwing, S. Campagna S.R., Steadman D.W., DeBruyn J.M. (2022) Body mass composition (BMI) impacts soil chemical and microbial responses during human decomposition. Abstract accepted as a poster presentation for the 2022 Academy of Forensic Sciences annual meeting (Seattle, WA). February 24, 2022.

McKee-Zech H.S., Owings C.G., Höland K., Patrick E., Schwing S., Delgado T., Campagna S., Steadman D.W. (2021) Human postmortem toxicological impacts on blow fly larval diversity and length. Entomological Society of America annual meeting (Denver, CO), October 2021. **virtual presentation due to COVID-19*

Owings C.G., McKee-Zech H.S., Patrick E., Schwing S., Delgado T., Steadman D.W. (2021) Quantifying the pre-colonization interval with human remains. Entomological Society of America annual meeting (Denver, CO), October 2021. **virtual presentation due to COVID-19*

McKee-Zech H.S., Owings C.G., Steadman D.W. (2021) State record and continued surveillance of the oriental latrine fly at the Anthropology Research Facility, Knoxville,

TN. Entomological Society of America annual meeting (Denver, CO), October 2021. **virtual poster presentation due to COVID-19*

Owings C.G., McKee-Zech H.S., Patrick E., Schwing S., Delgado T., Steadman D.W. (2021). Not all flies are created equal: Accuracy of time of placement estimations is species dependent. North American Forensic Entomology Association annual meeting, July 2021. **Virtual presentation due to COVID-19*

May A., Höland K.M., McKee H.S., Mason A.R., Schwing S., Owings C.G., Delgado T., Davis M.C., Zaretzki R.L., DeBruyn J.M., Steadman D.W., Campagna S.R. (2021) Using metabolomics to gain a deeper understanding of human decomposition. Poster presented at the American Academy of Forensic Sciences, February 18, 2021. **Virtual presentation due to COVID-19*

Mason A.R., McKee-Zech H.S., Höland K.M., Davis M.C., Schwing S., Delgado T., Steadman D.W., Campagna S.R., DeBruyn J.M. (2021) Inter-individual variation in soil chemistry and microbial ecology during human decomposition. Poster presented at the American Academy of Forensic Sciences, February 19, 2021. **Virtual presentation due to COVID-19*

Höland K.M., Campagna S.R., May A., McKee H.S., Davis M.C., Schwing S., Delgado T., Owings C.G., Mason A.R., DeBruyn J.M., Steadman D.W., Zaretzki R.L. (2021) Expanding frontiers in postmortem toxicology: Drug tracing in different postmortem matrices during human decomposition using ultra high-performance liquid chromatography–high-resolution mass spectrometry (UHPLC-HRMS). Poster presented at the American Academy of Forensic Sciences, February 17, 2021. **Virtual presentation due to COVID-19*

Steadman D.W., DeBruyn J.M., Owings C.G., Campagna S.R. (2021). Inter-Individual Variation in Soil Chemistry and Microbial Ecology During Human Decomposition. Paper presented at the National Institute of Justice Forensic Science Research and Development Symposium, February 16, 2021. **Virtual presentation due to COVID-19*

McKee H.S., Owings C.G., Höland K.M., Schnieder L., Mason A.R., Bugajski K., Campagna S.R., DeBruyn J.M., Steadman D.W. (2020) Prescription drugs detected in humans postmortem impact on *Phormia regina* Meigen (Diptera: Calliphoridae) larval length. Oral presentation given at the 2020 Entomological Society of America annual meeting, November 2020. **Virtual presentation due to COVID-19*

Mason A.R., McKee H.S., Höland K.M., Schwing S., Delgado T., DeBruyn J.M., Steadman D.W., Campagna S.R. (2020) Assessment of variability in soil chemistry and microbial ecology during early stages of human decomposition. American Society for Microbiology Microbe Meeting. 18-22 June 2020. **Virtual presentation due to COVID-19*

DeBruyn J.M. (2020) Soil signatures of decomposition. Panel (virtual) presentation for: Interdisciplinary Colloquium: In the Footprints of Colonia Dignidad, Chile: Pending Challenges for philosophy, history and forensic science. 9 Sept 2020 https://youtu.be/X65l-AOtFag **Virtual presentation due to COVID-19*

Mason A.R., McKee H.S., Höland K.M., Schwing S.T., Delgado T., DeBruyn J.M., Steadman D.W., Campagna S.R. 2020. Variability in soil chemistry and microbial ecology during human decomposition. Soil Science Society of America Soils meeting. 8-11 November 2020. **Virtual presentation due to COVID-19*

Höland K.M., Campagna S.R., Steadman D.W., DeBruyn J.M., McKee H., Mason A.R., May A., Delgado T., Schwing S. (2020) Utilizing metabolomics toward time-dependent metabolite monitoring in different postmortem specimens during human decomposition. Poster presented at the 72nd annual scientific meeting of the American Academy of Forensic Sciences, Anaheim, CA, February 21, 2020.

Dissertation

Höland K.M. (2021) Investigating the Potential of Postmortem Metabolomics in Mammalian Decomposition Studies in Outdoor Setting. Ph.D. Dissertation, Department of Chemistry, University of Tennessee.

References Cited

Banerjee, S., et al., *Opioid-induced gut microbial disruption and bile dysregulation leads to gut barrier compromise and sustained systemic inflammation.* Mucosal Immunology, 2016. 9(6): p. 1418-1428.

Bourel B., Tournel G., Hedouin V., Deveaux M., Goff M.L., and Gosset D. (2001). Morphine extraction in necrophagous insects remains for determining ante-mortem opiate intoxication. *Forensic Science International* 120:127–131.

Byrd J.H. and Allen, J.C. (2001). The development of the black blow fly, *Phormia regina* (Meigen). *Forensic Sci Int, 120*(1), 79-88.

Caracciolo A. B., Topp E. and Grenni P. (2015). Pharmaceuticals in the environment: Biodegradation and effects on natural microbial communities. A review. *Journal of Pharmaceutical and Biomedical Analysis* 106: 25-36.

Carvalho L.M., Linhares A.X., and Trigo J.R. (2001). Determination of drug levels and the effect of diazepam on the growth of necrophagous flies of forensic importance in southeastern Brazil. *Forensic Science International* 120(1-2):140-144.

Center for Disease Control (CDC). 2017. Health United States Report 2016. Centers for Disease Control and Prevention, National Center for Injury Prevention and Control, Division of Unintentional Injury Prevention. https://www.cdc.gov/drugoverdose/data/overdose.html accessed 18 Dec 2017.

Chai G., Governale L., Mcmahon A.W., Trinidad J.P., Staffa J., and Murphy D. (2012). *Trends of Outpatient Prescription Drug Utilization in US Children, 2002-2010*. Pediatrics. 130(1):23-31.

Damann F.E., Williams, D.E. and Layton, A.C. (2015). Potential use of bacterial community succession in decaying human bone for estimating postmortem interval. *Journal of forensic sciences*, *60*(4), pp.844-850.

Dautartas A., Kenyhercz M.W., Vidoli G.M., Jantz L.M., Mundorff A.Z. and Steadman D.W. (2018) Differential decomposition among pig, rabbit and human subjects. *Journal of Forensic Sciences* 63(6):1673-1683. PMID 29603225 DOI: 10.1111/1556-4029.13784 (2018)

DeBruyn J.M., Hoeland K., Taylor L.S., Stevens J.D., Moats M.A., Bandopadhyay S., Dearth S.P., Castro H.F., Hewitt K.K., Campagna S.R., Dautartas A.M., Vidoli G.M., Mundorff A.Z. and Steadman D.W. (2021) Comparative decomposition of humans and pigs: Soil biogeochemistry, microbial activity and metabolomic profiles. Frontiers in Microbiology 11:608856. doi:10.3389/fmicb.2020.608856

Deel H., Bucheli S., Belk A., Ogden S., Lynne A, Carter D.O., Knight R. and Metcalf J.L. (2020) Chapter 12 - Using microbiome tools for estimating the postmortem interval. In: Budowle B, Schutzer S, and Morse S, eds. *Microbial Forensics (Third Edition)*: Academic Press, 171-191.

Flores M., Crippen T.L., Longnecker M., and Tomberlin J.K. (2017). Nonconsumptive effects of predatory Chrysomya rufifacies (Diptera: Calliphoridae) larval cues on larval Cochliomyia macellaria (Diptera: Calliphoridae) growth and development. *Journal of Medical Entomology, 54*(5), 1167-1174.

Fuyuan W. and Sabita R. (2016) *Gut Homeostasis, Microbial Dysbiosis, and Opioids.* Toxicologic Pathology, 45(1): p. 150-156.

Gallagher M.B., Sandhu, S., and Kimsey, R. (2010) Variation in developmental time for geographically distinct populations of the common green bottle fly, *Lucilia sericata* (Meigen). *J Forensic Sci, 55*(2), 438-442. doi:10.1111/j.1556-4029.2009.01285.x

George K.A., Archer M.S., Green L.M., Conlan X.A., Toop T. (2009) Effect of morphine on the growth rate of *Calliphora stygia* (Fabricius) (Diptera: Calliphoridae) and possible implications for forensic entomology. *Forensic Sci Int* 193:21–25

Goff M.L., Omori A.I., and Goodbrod J.R. (1989). Effect of Cocaine in Tissues on the Development Rate of Boettcherisca peregrina (Diptera: Sarcophagidae). *Journal of Medical Entomology* 26(2):91-3.

Goodbrod J R., and Goff, M.L. (1990). Effects of larval population density on rates of development and interactions between two species of Chrysomya (Diptera: Calliphoridae) in laboratory culture. *Journal of Medical Entomology, 27*(3), 338-343.

Hales C.M., Kit, B.K., Gu, Q. and Ogden, C.L. (2018) Trends in prescription medication use among children and adolescents—United States, 1999-2014. *Jama, 319*(19), pp.2009-2020.

Hayman J. and Oxenham M. (2016). Peri-mortem disease treatment: a little known cause of error in the estimation of the time since death in decomposing remains. *Australian Journal of Forensic Sciences* 48(2):171-185.

Huang Y., Pinto, M.D., Borelli, J.L., Mehrabadi, M.A., Abrihim, H., Dutt, N., Lambert, N., Nurmi, E.L., Chakraborty, R., Rahmani, A.M., and Downs, C.A. (2021) COVID symptoms, symptom clusters, and predictors for becoming a long-hauler: Looking for clarity in the haze of the Pandemic. *medRxiv : the preprint server for health sciences*, 2021.03.03.21252086. https://doi.org/10.1101/2021.03.03.21252086

Kintz P., Godelar A., Tracqui A., Mangin P., Lugnier A.A., Chaumont A.J. (1990). Fly larvae: a new toxicological method of investigation in forensic medicine. *Journal of Forensic Sciences* 35:243–246.

Kochanek K.D., Xu J.Q., Arias E. (2020) Mortality in the United States, 2019. NCHS Data Brief, no 395. Hyattsville, MD: National Center for Health Statistics. https://www.cdc.gov/nchs/products/databriefs/db395.htm

Liu, D.; Greenberg, B. (1989) Immature stages of some flies of forensic importance. *Annals of the Entomological Society of America 82* (1), 80-93.

Mann, R.W., Bass, W.M. and Meadows, L. (1990) Time since death and decomposition of the human body: variables and observations in case and experimental field studies. *Journal of Forensic Science*, *35*(1), pp.103-111.

Megyesi M.; Nawrocki, S.; Haskell, N. (2005) Using accumulated degree-days to estimate the postmortem interval from decomposed human remains. *Journal of Forensic Sciences 50* (3), 1-9.

Metcalf J, Wegener Parfrey L, Gonzalez A, Lauber C, Knights D, Ackermann G, Humphrey G, Gebert M, Van Treuren W, Berg-Lyons D, Keepers K, Guo Y, Bullard J, Fierer N, Carter D, and Knight R. (2013) A microbial clock provides an accurate estimate of the postmortem interval in a mouse model system. *eLife* 2:e01104. 10.7554/eLife.01104

National Institute of Drug Abuse. (2020 July 9). Substance Use in Older Adults Drug Facts. Retrieved from https://www.drugabuse.gov/publications/substance-use-in-older-adults-drugfacts on 2021, August 26.

Owings C.G., Mckee-Zech H., and Steadman D.W. (2021). First record of the oriental latrine fly, Chrysomya megacephala (Fabricius)(Diptera: Calliphoridae), in Tennessee, USA. *Acta Parasitologica*, 1-3.

Owings C., Spiegelman C., Tarone A., and Tomberlin, J. (2014). Developmental variation among *Cochliomyia macellaria* Fabricius (Diptera: Calliphoridae) populations from three ecoregions of Texas, USA. *Internat J Legal Med, 128*(4), 709-717. doi:10.1007/s00414-014-1014-0

Pechal J.L., Crippen T.L., Benbow M.E., Tarone A.M., Dowd S., and Tomberlin J.K. (2014) The potential use of bacterial community succession in forensics as described by high throughput metagenomic sequencing. *Internat J Legal Med* 128:193-205.

Picard C. and Wells, J. (2009). Survey of the genetic diversity of *Phormia regina* (Diptera: Calliphoridae) using Amplified Fragment Length Polymorphisms. *J Med Entomol, 46*(3), 664-670.

Picard C. and Wells, J. (2010). The population genetic structure of North American *Lucilia sericata* (Diptera: Calliphoridae), and the utility of genetic assignment methods for reconstruction of postmortem corpse relocation. *Forensic Sci Int, 195*(1–3), 63-67. doi:http://dx.doi.org/10.1016/j.forsciint.2009.11.012

Picard C.J., Deblois K., Tovar F., Bradley J.L., Johnston J.S., and Tarone A.M. (2013). Increasing precision in development-based postmortem interval estimates: what's sex got to do with it? *Journal of Medical Entomology, 50*(2), 425-431.

Qin Q., Chen X.J. and Zhuang J. (2015). The fate and impact of pharmaceuticals and personal care products in agricultural soils irrigated with reclaimed water. *Critical Reviews in Environmental Science and Technology* 45(13): 1379-1408.

Rodriguez W.C. and Bass W.M. (1983) Insect activity and its relationship to decay rates of human cadavers in East Tennessee. *Journal of forensic science*, *28*(2), pp.423-432.

Rodriguez W.C. and Bass W.M. (1985) Decomposition of buried bodies and methods that may aid in their location. *Journal of Forensic Science, 30*(3), pp.836-852.

Steadman D.W., Dautartas A., Kenyhercz M.W., Jantz L.M., Mundorff A., and Vidoli G.M. (2018) Differential scavenging among pig, rabbit, and human subjects. *Journal of Forensic Sciences* 63:1684-1691. 10.1111/1556-4029.13786

Szpila K. (2009) Key for the identification of third instars of European blowflies (Diptera: Calliphoridae) of forensic importance. In *Current concepts in forensic entomology* (pp. 43-56). Springer, Dordrecht.

United Nations Office on Drugs and Crime, 2021. World Drug Report. https://www.unodc.org/unodc/en/data-and-analysis/wdr2021.html. Accessed 21 August 2021.

Vass A.A., Bass W.M., Wolt J.D., Foss J.E. and Ammons J.T. (1992). Time since death determinations of human cadavers using soil solution. *Journal of Forensic Science*, *37*(5), pp.1236-1253.

Visser S.N., Danielson M.L., Bitsko R.H., Holbrook J.R., Kogan M.D., Ghandour R.M., Perou R. and Blumberg S.J. (2014) Trends in the parent-report of health care provider-diagnosed and medicated attention-deficit/hyperactivity disorder: United States, 2003–2011. *Journal of the American Academy of Child & Adolescent Psychiatry*, *53*(1), pp.34-46.

Wells J.D. and Greenberg B. (1992). Interaction between Chrysomya rufifacies and Cochliomyia macellaria (Diptera: Calliphoridae): the possible consequences of an invasion. *Bulletin of Entomological Research, 82*(01), 133-137.

Wells J.D. and Greenberg B. (1994). Resource use by an introduced and native carrion flies. *Oecologia, 99*(1-2), 181-187.

Wilson-Taylor, R.J. and Dautartas, A.M. (2017) Time since death estimation and bone weathering: The postmortem interval. In *Forensic Anthropology* (pp. 291-330). CRC Press.

Appendix I – Donor Demography, Medical Conditions and Medications

TOXID	SEX	AGE	ANCESTRY	STATURE (CM)	WEIGHT (LB)	Cause of Death	Medical Conditions	Medications
TOX001	F	63	White	170.5	214	Coronary Artery Disease, Diabetes, Hypertension	Asthma, COPD, Diabetes, Hypothyroidism, Multiple Sclerosis, GERD, IBS, Chronic Kidney Disease, Ovarian Cancer, ASCVD, Coronary Artery Disease, Hypertension, Hypercalcemia, Vitamin D Deficiency, Depression, Tobacco Use	Albuterol, Amlodipine, Atorvastatin, Carvedilol, Clopidogrel, Cymbalta, Gabapentin, Lantus, Levothyroxine, Lisinopril, Nitroglycerin, Novolog, Oxybutynin, Pantoprazole, Trelegy
TOX002	F	78	White	162	117	Colon Cancer	Hypothyroidism, Colon Cancer, Depression, Tobacco Use, Alcohol Abuse	Aspirin, Atorvastatin, Digoxin, Levothyroxine, Losartan, Paroxetine, Tizanidine, Valium, Xanax
TOX003	M	71	White	170	127	COPD	COPD, Pancreatitis, Tobacco Use, Alcohol Abuse	Med List Not Obtained
TOX004	F	84	White	147	92	Lung Cancer	Lung Cancer, Tobacco Use	Haldol, Lidocaine, Lorazepam, Morphine
TOX005	F	71	White	157	126	Pneumonia, Adult Respiratory Distress Syndrome	Pneumonia, Adult Respiratory Distress Syndrome, Breast Cancer	Acetaminophen, Albuterol, Amlodipine, Atenolol, Calcium-Vitamin D, Enoxaparin, Famotidine, Furosemide, Ibuprofen, Iron, Letrozole, Levothyroxine, Lorazepam, Morphine, Omeprazole, Ondansetron, Oxycodone, Palbociclib, Pantoprazole, Sodium Chloride

This resource was prepared by the author(s) using Federal funds provided by the U.S. Department of Justice. Opinions or points of view expressed are those of the author(s) and do not necessarily reflect the official position or policies of the U.S. Department of Justice.

TOXID	SEX	AGE	ANCESTRY	STATURE (CM)	WEIGHT (LB)	Cause of Death	Medical Conditions	Medications
TOX006	M	64	White	162	144	Lymphoma, Renal Failure, Stroke, Heart Disease	COPD, Chronic Renal Failure, Lymphoma, Peripheral Artery Disease, Stroke, Tobacco Use	Allopurinol, Atorvastatin, Buspirone, Citalopram, Eliquis, Furosemide, Hydrocodone-Acetaminophen, Klor-Con, Lorazepam, Metoprolol
TOX007	M	89	White	179	185	Congestive Heart Failure	CHF, Stroke, Tobacco Use	Aspirin, Furosemide, Lisinopril, Metoprolol, Warfarin
TOX008	M	40	White	160	137	Leukemia	Ulcers, Leukemia, Stroke	Gabapentin, Ondansetron, Oxycodone, Ponatinib, Ranitidine, Warfarin
TOX009	F	72	White	158	131	Lung Cancer	Lung Cancer, Tobacco Use	Albuterol, Atropine, Hyoscyamine, Lorazepam, Metoprolol, Morphine, Ondansetron, Scopolamine, Sodium Chloride
TOX010	M	65	White	177	374	COPD, Hypertension, Pneumonia	COPD, Pneumonia, Diabetes, Hypertension	Med List Not Obtained
TOX011	M	81	White	170	140	Parkinson's Disease	Kidney Cancer, Stroke, Parkinson's Disease	Acetaminophen, Bisacodyl, Hyoscyamine, Lorazepam, Morphine, Prochlorperazine
TOX012	F	77	White	154	154	Renal Disease, Seizures, TIA, Diabetes, Cerebral Hemorrhage	Diabetes, Hyperparathyroidism, Chronic Kidney Disease, Stroke, Dementia, Seizures	Albuterol, Aspirin, Buspirone, Cymbalta, Gabapentin, Geodon, Haldol, Ibuprofen, Lantus, Lisinopril, Lorazepam, Morphine, Voltaren
TOX013	M	54	White	174	278	Asphyxia via Ligature Hanging	Migraines, Depression, Sleep Apnea, Erectile Dysfunction	Ambien, Imitrex, Sildenafil

TOXID	SEX	AGE	ANCESTRY	STATURE (CM)	WEIGHT (LB)	Cause of Death	Medical Conditions	Medications
TOX014	M	74	White	190	198	Hepatocellular Carcinoma, Atrial fibrillation, Hypertension	Seasonal Allergies, Lupus, Cirrhosis, Liver Cancer, Aortic Stenosis, Atrial Fibrillation, Hypertension, Hyperlipidemia, Tobacco Use	Med List Not Obtained
TOX015	M	78	White	164	84	Pulmonary Fibrosis	Diabetes, Hypertension, Pulmonary Fibrosis	Acetaminophen, Colace, Fentanyl, Glimepiride, Guaifenesin, Hydrocodone-Acetaminophen, Levothyroxine, Lorazepam, MiraLax, Morphine, Ondansetron
TOX016	M	62	White	184	280	Chronic Hypoxic and Hypercapnic Respiratory Failure, Advanced COPD, Obstructive Sleep Apnea	COPD, Seasonal Allergies, GERD, Skin Cancer, Congestive Heart Failure, Peripheral Artery Disease, Stroke, Hypertension, Hyperlipidemia, Depression, Tobacco Use, Alcohol Abuse	Albuterol, Clonidine, Clopidogrel, Hydrochlorothiazide, Lisinopril, Meloxicam, Metoprolol, Omeprazole, Pantoprazole, Spironolactone
TOX017	F	62	White	160	311	Congestive Heart Failure	Diabetes, Hypothyroidism, GERD, Constipation, Uterine Cancer, Congestive Heart Failure, Ventricular Hypertrophy, TIA, DVT, Hypertension, Hyperlipidemia, Vitamin B12 Deficiency, Hypomagnesemia, Anemia, Bipolar Disorder, Insomnia, Paroxysmal Nocturnal Dyspnea, Benzodiazepine Dependence, Opiate Dependence, Restless Leg Syndrome, Rosacea	Albuterol, Amlodipine, Aspirin, Belsomra, Bevespi Aerosphere, Clonazepam, Colace, Eliquis, Ezetimibe, Furosemide, Hydrocodone-Acetaminophen, Iron, Januvia, Levothyroxine, Lidocaine, Magnesium, Mirapex, Montelukast, Myrbetriq, Omeprazole, Promethazine, Sodium Chloride, Trulicity, Xanax

TOXID	SEX	AGE	ANCESTRY	STATURE (CM)	WEIGHT (LB)	Cause of Death	Medical Conditions	Medications
TOX018	F	85	White	146	75	Parkinson's Disease	Parkinson's Disease	Acetaminophen, Atropine, Bactroban, Biofreeze Roll-On, Carbidopa-Levodopa, Escitalopram, Guaifenesin, Hydrocodone-Acetaminophen, Hyoscyamine, Milk of Magnesia, Senna
TOX019	F	67	White	152	100	Lung Cancer	Hypothyroidism, Breast Cancer, Lung Cancer, Tobacco Use	Atorvastatin, Cyclobenzaprine, Dexamethasone, Haldol, Hydrocodone-Acetaminophen, Ibuprofen, Lamotrigine, Levothyroxine, Lorazepam, Morphine, Omeprazole, Ondansetron, Promethazine, Ropinirole
TOX020	M	91	White	164	185	Respiratory Failure, Emphysema	COPD, Emphysema, Seasonal Allergies, Diabetes, GERD, Chronic Kidney Disease, Prostate Cancer, Coronary Artery Disease, Hypertension, Hyperlipidemia, Insomnia, Tobacco Use, Alcohol Abuse	Acetaminophen, Albuterol, Bisacodyl, Famotidine, Flutamide, Furosemide, Haldol, Hydralazine, Hydromorphone, Hyoscyamine, Isosorbide, Mononitrate, Lorazepam, Metoprolol, Ondansetron, Senna, Tramadol, Xanax

TOXID	SEX	AGE	ANCESTRY	STATURE (CM)	WEIGHT (LB)	Cause of Death	Medical Conditions	Medications
TOX021	M	71	White	162.5	211	Acute Respiratory Failure	Acute Kidney Injury, Alcohol Abuse, Ascites, ASCVD, Congestive Heart Failure, COPD, Gout, Stroke, Tobacco Abuse	Med list not obtained
TOX022	F	60	White	155	199	Blunt force trauma	Bipolar, Diabetes, Hypertension, Schizophrenia	Med list not obtained